journal of the international meteor organization

WGN

48:4
august 2020

Problems in searching for meteor showers

Enhanced radio detectability of meteor head echoes passing zero Doppler shift

Frequency shifts of head echoes in meteoroid trail formation

Beliefs: was Mithras really 'born' from a meteorite?

ISSN 1016-3115

WGN Vol. 48, No. 4, August 2020, pp. 99 – 128

Meteor science

Radio meteors

Meteor Beliefs

Front and back cover photo

Composite image of the 2020 Perseids maximum, using photographs taken from Poloniny National Park in Slovakia during four nights from 2020 August 9 to 13. The author used two identical Canon 6D cameras employing Samyang 12-mm and 28-mm lens to take 5431 images. The final composite image contains 148 meteors. Photo courtesy: Tomaš Slovinský.

Writing for WGN

This Journal welcomes papers submitted for publication. All papers are reviewed for scientific content, and edited for English and style. Instructions for authors can be found in WGN **45:1**, 1–5, and at `http://www.imo.net/docs/writingforwgn.pdf` .

Legal address

International Meteor Organization, Jozef Mattheessensstraat 60, 2540 Hove, Belgium.

Meteor science

Problems in Searching for Meteor Showers

Masahiro Koseki[1]

D-criteria are useful when searching for similar orbits but several problems can occur when searching for meteor showers on the basis of these similarities. Some hundred thousands of video meteor orbit data have been published and we can find meteors having nearly identical orbits easily. Here we study problems of *D*-based meteor shower research in the case of BRAMON's new method (Amaral et al., 2019).
1. Excluding "shower meteors" by using the classification of the source data lead to erroneous findings, because the classifications are widely different from each other.
2. "Break-point" is a useful index for defining meteor shower activity from background sporadics, but it is valid only for major showers, that is, abundant shower meteors relative to the background.
3. Cluster analysis such as DBSCAN needs the distance measure and it is difficult to find an appropriate value; especially in the case of the vicinity to a major shower.
It becomes clear that additional RP-based study (see the text) is necessary to confirm new shower activities. There are many methods for searching meteor showers and there are various conceptions of "a meteor shower/meteoroid stream", but the results should be confirmed by different methods in order to be verified as new showers by the world. This paper presents the problems in the search, especially using *D* criteria methods.

Received 2020 June 15

1 Observational raw data or calculated orbital elements?

We can get meteor data by observations firstly and convert them into orbital elements easily. We can, then, search new meteor showers by using them; observational raw data (RP-based) and the orbital elements (OE-based). They have four independent values: RP-based studies have the position of the radiant point (α, δ), the velocity and the time of the appearance while OE-based studies have the size and shape of an orbit, the orientation of the perihelion and the angle of the Earth's orbit crossing. The terms meteor shower and meteoroid stream are not the same but we use only meteor shower hereafter except if it is necessary to distinguish them.

Researchers have used these two attempts in different ways. For example, Sekanina (1970) used OE-based and Brown et al. (2008) used RP-based searches. Sekanina used $D_{\rm SH}$ (Southworth and Hawkins, 1963) distributions and Brown et al. used their wavelet program. The author showed there are many definitions to search meteor showers/streams (Koseki, 2014) and the results might be different for even one and the same data. RP-based and OE-based studies both depend on their own warped four dimensional space in order to find a concentration of meteors. First, we look at the data of the Capricornids as an example to demonstrate the difference between them.

1.1 D-criteria based studies

Galligan (2001) compared several D-criteria and showed they have different cut-off levels for retrieving meteoroid stream members. He concluded "Southworth & Hawkins's (1963) $D_{\rm SH}$ is also found to function competently" and "$D_{\rm SH}$ will be apt to efficiently retrieve streams at different inclinations". We use $D_{\rm SH}$ as an example to show how a *D*-criterion works on meteor shower search taking Galligan's suggestion into consideration.

Sekanina (1970) presented an idea to detect meteor activity from sporadic background using the $D_{\rm SH}$ distribution. Figure 1a shows the $D_{\rm SH}$ distribution of the 0001CAP08 (IAU 4 digit number + 3 character code + AdNo.) and Figure 1b shows the cumulative $D_{\rm SH}$ distribution in a logarithmic scale using SonotaCo network data (SonotaCo, 2009). We can notice a small mound near the y-axis followed by long ascent. This represents the CAP activity which is better expressed by Figure 1b. The broken line in Figure 1b is ended from the regression between $D_{\rm SH} = 0.04$ and 0.1; it seems to represent the sporadic background. We can, therefore, estimate the real activity of the CAP with the $D_{\rm SH}$; Figure 1c shows the difference between the curve and the straight line in Figure 1b in real numbers. *D*-criteria show the meteor distribution in a four dimensional space: shape, size, orientation and crossing angle. The meteor densities in the four dimensional space for CAP are shown in Figure 1d; the solid line is the partial density each $\Delta D_{\rm SH} = 0.01$ and the dashed line is the total density, i.e. the cumulative number divided by the space of the indicated $D_{\rm SH}$.

1.2 Radiant based studies

We can show a meteor distribution in another way, giving the radiant point (α, δ), date and velocity. It is clear that a radiant distribution should be described in $(\lambda - \lambda_s, \beta)$ rather than in (α, δ) because the former may eliminate the radiant shift largely. Figure 1e gives, therefore, the radiant distribution of $D_{\rm SH} < 2$ in $(\lambda - \lambda_s, \beta)$ and it is clear that a $D_{\rm SH}$ study is equivalent to a radiant based study.

[1]Nippon Meteor Society (NMS), 4-3-5 Annaka, Annaka-shi, Gunma-ken, 379-0116, Japan.
Email: geh04301@nifty.ne.jp

IMO bibcode WGN-484-koseki-search
NASA-ADS bibcode 2020JIMO...48...99K

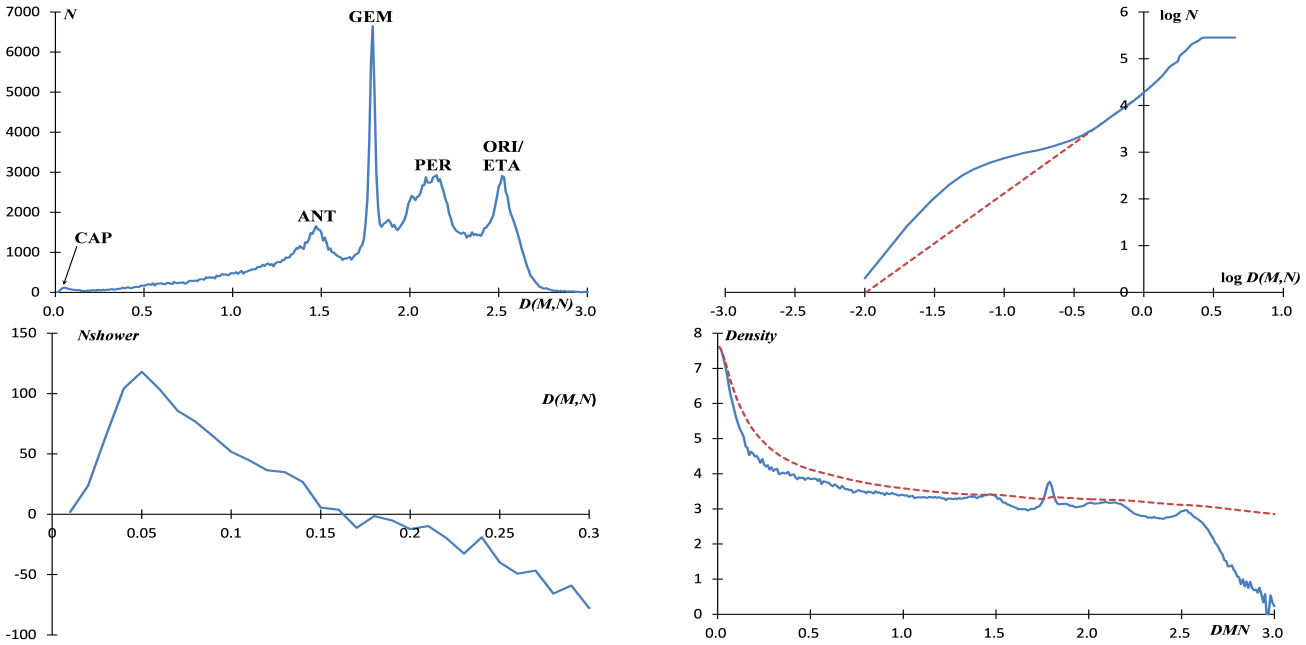

Figure 1 – (a)–(d) **The Capricornids as an example:** OE-based results (a)–(e) and (h) are calculated from 0001CAP08 and RP-based studies; (f) and (g) are from 0001CAP04 as basic data.
(a) $D_{\rm SH}$ distribution: the mound of Capricornids is indicated by an arrow. Several major showers (GEM, PER, ORI and ETA) and the Antihelion source (ANT) produce various peaks. These peaks would move when we choose another shower for the calculation (top left).
(b) Cumulative $D_{\rm SH}$ distribution as logarithmic plot. The small mound in Figure 1a is magnified by the logarithmic expression. The sporadic background estimated from $0.40 < D_{\rm SH} < 1.0$ is indicated by the dashed line (top right).
(c) Estimated Capricornid distribution shown as real numbers: the difference between the straight line and the dashed line of Figure 1b. The small mound is represented by the subtraction of estimated sporadics from the total number (2nd left).
(d) Estimated $D_{\rm SH}$ density in the four dimensional $D_{\rm SH}$ space, i.e., the number of meteoroids in the unit volume in the four dimensional space: the solid line is the partial density each $\Delta D_{\rm SH} = 0.01$ bin and the dashed line is the total density, i.e. the cumulative number divided by the total volume of the indicated $D_{\rm SH}$.

The author investigated several showers by a radiant based study (Koseki, 2019b) and he gave the radiant distribution of the CAP in different views: in (α, δ), in $(\lambda - \lambda_s, \beta)$, in $(\lambda - \lambda_s, \beta)$ including the radiant shift estimation. Figure 1f shows the shift compensated CAP radiant distribution between $\lambda_\odot = 117\overset{\circ}{.}9 < \lambda_s < 137\overset{\circ}{.}9$ using the radiant point of the 0001CAP04 $(\lambda - \lambda_s, \beta) = (179\overset{\circ}{.}3, 9\overset{\circ}{.}9)$ as reference. In a radiant based study, we can search for shower members taking the radiant shift into consideration which is not possible in a D value based study. The activity profile of CAP can be drawn by counting meteor numbers within 3° from the shift compensated radiant point (Figure 1g); $Nr \leq 3$ is the raw meteor number within 3°, $DR3$, $DR10$ and $DR15$ are the corrected number by the meteor numbers of the surrounding areas (see the caption of Figure 1g for details). It is suggested that the activity period of the CAP is between $110° < \lambda_s < 140°$, i.e. $DR > 5$ and $Nr \leq 3$ is larger than 5. Figure 1h shows the variation of $D_{\rm SH}$ between 0001CAP08 and the estimated orbital elements by using the radiant shift compensation (the right axis DMN) and $DR15$ (left axis) as given in Figure 1g. We realize that the activity period of CAP is corresponding to $D_{\rm SH} < 0.2$.

2 Case study: BRAMON's new meteor showers

Amaral et al. presented new technique to search for meteor showers (Amaral et al., 2018). They reported 127 new radiants were detected and their results were included in the IAU meteor shower database (SD) under pro-tempore status by the working group. The radiants are rejected from the recent SD because their results had not been published yet. Therefore we use the SD of 2018 Jan 13 20:35:17 version which has BRAMON's showers included.

Here, the author checked all the reported new 'radiants' by a radiant based study (Koseki, 2020a) but can recognize possible activity only for 9 of 127 entries listed in Table 1. These are the radiants 0814CVD00, 0919ICN00, 0937FOD00, 0958SXS00, 0972JGL00, 0984OST00, 0986SAD00, 0994DBC00 and 1002SVE00. It seems interesting to find out why such differences occur. We select several of these 'radiants' and check them by applying an OE based analysis.

2.1 November Cetids (0799NEC00)

The $D_{\rm SH}$ distribution shows that the NEC activity is almost buried under the sporadic background (Figure 2a). If we select meteors $D_{\rm SH} < 0.4$ as NEC meteors, the respective activity profile is shown as Figure 2b. The profile suggests that the NEC is active longer

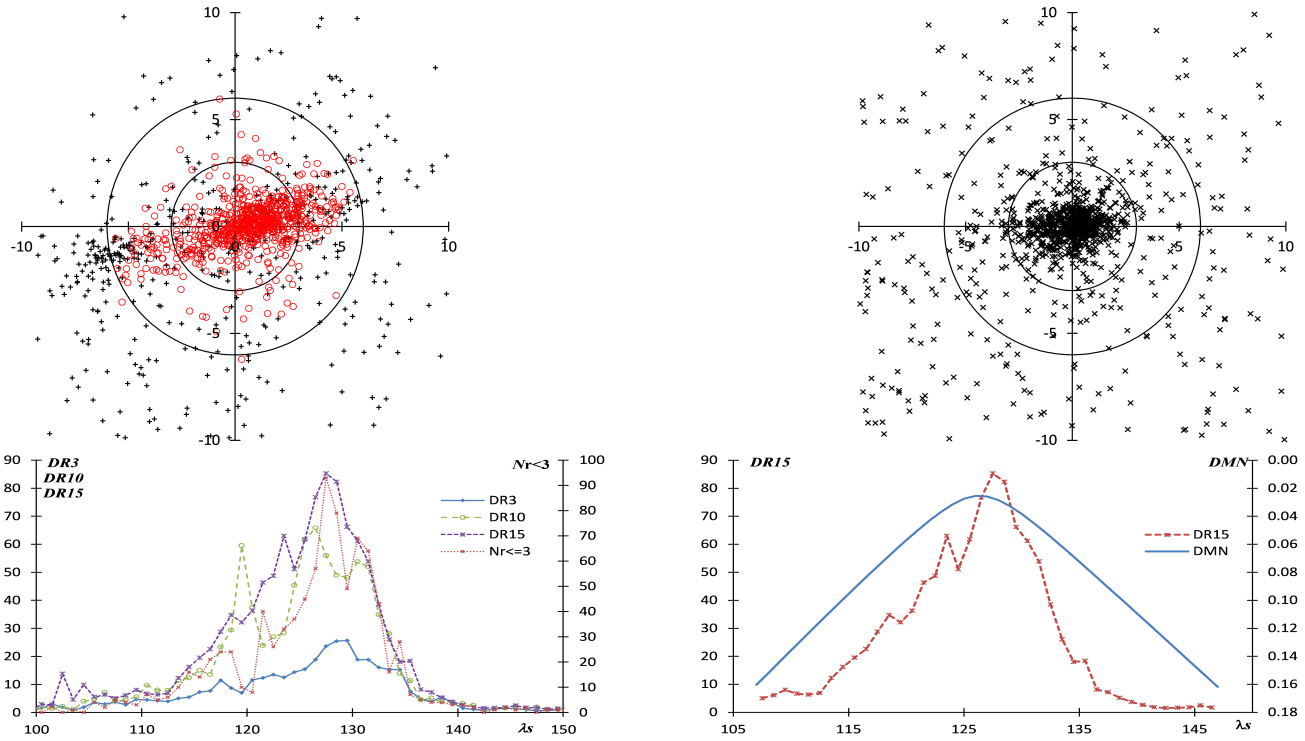

Figure 1 – (e)–(h): (e) Radiant distribution of Capricornids selected within $D_{\rm SH} < 0.20$ for 0001CAP08: circles $D_{\rm SH} < 0.10$, plus sign $0.10 < D_{\rm SH} < 0.20$. Circles show elongated distribution suggesting radiant shift with time. (top left).
(f) Radiant distribution of Capricornids corrected for the radiant shift used meteors between $117\overset{\circ}{.}9 < \lambda_s < 137\overset{\circ}{.}9$. Radiants show circular distribution indicating the elongated distribution in Figure 1e is caused by the radiant shift. (top right).
(g) The activity profile of Capricornids taking the radiant shift into consideration. $Nr \leq 3$ is the number of meteors within 3° from the estimated radiant in each 1° bin of λ_s; $DR3$ is the density ratio within a circle of 3° radius relative to a ring of $3-6^\circ$; $DR10$ is the density ratio within a circle of 3° relative to a ring of $6-10^\circ$; $DR15$ is the density ratio within a circle of 3° relative to a ring of $10-15^\circ$. It is better to use the sliding mean of the radiant density ratios within bins of 3° in λ_s in order to avoid shortages of meteor numbers in the reference areas. (bottom left).
(h) The change of $D_{\rm SH}$ values for the estimated orbital elements taking the radiant shift into consideration to 0001CAP08. The estimated elements are calculated from the linear regression of radiant points on $(\lambda - \lambda_s, \beta)$ coordinates and of geocentric velocity. Figure 1f is the result of the several iterations of the linear regression of radiant points. The dashed line is the same as $DR15$ in Figure 1g.

than the Taurids. We can draw a radiant distribution of NEC $D_{\rm SH} < 0.4$ meteors as shown Figure 2c. There are 48 meteors of $D_{\rm SH} < 0.1$ but they do not show any concentration.

2.2 July Cetids (0800JCT00)

JCT seems to be a chance association of sporadic meteors. Figure3a shows that the meteor distribution is identical to that of sporadics. 284 meteors were on orbits with $D_{\rm SH} < 0.4$ and the radiant distribution of them represents a typical sporadic one (Figure 3c), though the activity profile seems as if there was a meteor shower activity (Figure 3b).

2.3 26 Cetids (0929TXC00)

Looking at the $D_{\rm SH}$ distribution (Figure 4a), the TXC seems to be a candidate of a new shower. But Figure 4b shows that 'TXC' is a twin shower: the SD lists the activity of the ascending node ($\lambda_s = 134\overset{\circ}{.}6$) and this $D_{\rm SH}$ survey detects the other activity around the descending node at $\lambda_s = 314\overset{\circ}{.}6$. It is necessary to distinguish each activity to draw the radiant distribution. Figure 4c gives the one for the ascending node. It should be stressed that we need to check the existence of the twin when we use D-value based study for searching meteor showers.

2.4 17 Eridanids (1002SVE00)

SVE is a noticeable shower in the radiant based study ($Nr \leq 3$ is 7 and $DR15 = 9.0$ in Table 1). Figure 5a clearly shows that the 'break point' and meteors with $D_{\rm SH} < 0.2$ are concentrated around the center in Figure 5c. It is noteworthy to note the estimated number drops negative over $D_{\rm SH} > 0.2$ when we draw the real number distribution as shown in Figure 1c. We checked several major showers listed in Table 2 and found out such difference (the estimated number) becomes negative over $D_{\rm SH} > 0.2$ in many cases.

3 Discussion

The comparison between D value and radiant based studies reveals the problems in the meteor shower searches. Recent video technique has piled up some hundred thousand meteor orbits and more than one thousand meteor showers have been posted to the SD. We must reconsider the process how those showers have

Table 1 – The list of BRAMON's meteor showers with the RP-based study results. $Nr \leq 3$ gives the meteor number within 3° from the center ($\lambda - \lambda_s$, β) and $DR3$ is the density ratio of radiants within 3° from the center relative to the ring between 3° to 6° from the center. $DR3$ is the sliding mean of the radiant density ratio within bins of 3° degrees in λ_s in order to avoid shortages of meteor numbers in the reference areas. Both columns are followed by λ_s and max where max is the peak $Nr \leq 3$ or $DR3$ reached at their maximum λ_s. These RP-based results are given in the period 10 degrees before and after the given λ_s. In the remarks, a possible relation to other showers is given as the SD code of the shower/the code of the candidate/the distance between them in degrees.

Code	λ_s [°]	$\lambda - \lambda_s$ [°]	β [°]	$Nr <= 3$ λ_s [°]	max	DR3 λ_s [°]	max	Remarks
0799NEC00	233.6	135.6	−16.4	236.5	1	235.5	3.0	
0800JCT00	110.4	264.6	−14.7	108.5	2	100.5	6.0	
0801JCD00	88.7	280.1	−29.2	88.5	0	88.5	0.0	
0802ADS	90.8	237.6	−7.5	85.5	4	83.5	4.0	
0803LSA	75.25	201.2	−2.4	72.5	5	73.5	2.7	LSA1/069SSG0/2.76
0804DGR00	91.3	231.7	−31.8	91.5	0	91.5	0.0	
0805GSC00	86.6	251.0	−21.4	93.5	1	94.5	2.0	
0806SGI00	72.8	204.3	2.9	73.5	7	74.5	3.0	
0807FLO	330.8	195.4	−2.1	329.5	7	330.5	1.7	
0808PCS00	226.9	87.8	−3.0	218.5	1	218.5	3.0	
0809USG00	50.7	201.2	4.8	52.5	8	52.5	1.5	
0810XCD	187.3	210.1	−7.4	179.5	3	180.5	4.5	
0811LCP00	202.1	122.3	1.7	206.5	1	202.5	0.0	
0812NAA	232.19	211.0	23.4	238.5	3	238.5	9.0	
0813OAC00	213.6	217.3	43.2	213.5	2	224.5	4.0	
0814CVD	304.2	222.2	39.0	304.5	6	304.5	5.7	
0815UMS	155.95	327.9	45.8	160.5	1	159.5	3.0	
0816CVT	331.85	207.3	38.5	329.5	2	330.5	2.1	
0817PCI00	135.6	235.9	8.6	131.5	8	123.5	4.2	
0818OAG	205.15	228.0	13.4	207.5	6	206.5	3.6	
0819SPS00	182.3	239.3	27.7	183.5	4	187.5	2.4	
0820TRD00	192.4	237.6	−9.6	194.5	6	194.5	2.6	
0821DRP00	251.2	243.1	−42.5	248.5	3	249.5	3.5	
0919ICN	300.6	272.1	−27.7	297.5	6	299.5	5.1	
0929TXC00	134.6	241.7	−5.8	131.5	6	127.5	3.5	
0930NUC00	125.5	272.8	−7.7	123.5	4	119.5	4.5	
0931NFC00	131.2	276.4	−20.3	136.5	6	125.5	3.0	
0933CAV00	1.9	199.6	−1.7	7.5	8	359.5	3.7	
0934OAD00	172.8	225.6	32.6	172.5	2	175.5	4.5	
0935APO00	32	233.6	30.7	35.5	3	35.5	3.7	
0936STO00	208.8	246.7	−7.5	207.5	1880	208.5	31.6	coincides with 008ORI, over 15 km/s slower
0937FOD00	197.1	233.8	−20.2	208.5	5	185.5	5.0	
0938PEA00	139	283.4	37.0	139.5	2687	141.5	14.7	coincides with 007PER, about 15 km/s slower
0939EPA00	146	236.3	22.4	131.5	5	130.5	4.5	
0940FNA00	131.2	272.7	25.6	136.5	9	126.5	3.0	
0941MUT00	146.1	338.0	53.1	145.5	1	145.5	3.0	
0942EPE00	139.9	283.0	38.5	139.5	2968	139.5	26.1	coincides with 007PER, about 40 km/s slower
0943FTL00	314.8	195.0	19.9	316.5	2	323.5	6.0	
0944TGD00	262.8	198.8	12.3	262.5	36	272.5	2.5	located 10° west of 004GEM
0945SNC00	295.2	200.8	5.5	306.5	8	290.5	1.9	
0946TEA00	199.3	203.2	−3.2	193.5	10	181.5	4.2	TEA0/237SSA0/1.35
0947EPO00	206.6	236.3	−26.1	222.5	5	186.5	2.2	
0948SER00	171.3	231.1	−25.0	175.5	4	181.5	6.0	coincides with 849SZE
0949SGD00	262.3	208.2	10.6	262.5	8304	262.5	33.6	coincides with 004GEM, 10 km/s slower
0950FCS00	191.6	220.5	43.9	193.5	4	192.5	5.0	
0951OKH00	206.1	303.8	−30.7	202.5	1	202.5	3.0	
0952HNT00	163.9	277.1	−2.2	175.5	4	170.5	1.7	
0953ZGD00	192.8	272.1	−3.4	185.5	6	200.5	2.7	
0954NOL00	238.3	265.3	−2.9	221.5	8	229.5	2.1	
0955DIL00	275.6	236.1	−4.4	281.5	10	282.5	2.5	
0956SVD00	295.3	247.0	5.0	286.5	8	287.5	1.9	
0957SXT00	132.3	293.9	−6.9	134.5	3	145.5	4.0	
0958SXS00	25.6	243.1	7.6	23.5	5	33.5	9.0	SXS0/652OSP1/1.34
0959TLD00	204.4	296.7	−6.8	212.5	4	202.5	5.0	coincides with 877OHD
0960SEO00	166.6	276.7	−24.1	167.5	4	172.5	2.7	
0961FEL00	331.3	269.6	5.5	331.5	4	329.5	3.7	
0962ARO00	155.1	282.0	−18.8	167.5	8	151.5	3.6	
0963TOV00	315.6	237.5	−7.1	312.5	5	311.5	2.0	
0964NSD00	339.1	280.7	11.7	330.5	3	329.5	6.0	
0965FEA00	32.1	270.2	12.7	33.5	2	40.5	4.0	

Table 1 – (continued)

Code	λ_s [°]	$\lambda - \lambda_s$ [°]	β [°]	$Nr <= 3$ λ_s [°]	max	DR3 λ_s [°]	max	Remarks
0966TTP00	97.3	264.4	−6.8	91.5	2	90.5	6.0	
0967SSO00	352.6	277.2	27.6	351.5	6	356.5	3.7	
0968UOD00	4.8	241.9	11.8	1.5	4	9.5	2.2	coincides with 862SSR
0969EMD00	187.2	274.0	−19.6	206.5	5	190.5	3.0	
0970TOO00	340.5	270.5	24.2	332.5	8	346.5	2.6	
0971SIO00	9.4	251.5	30.0	11.5	3	17.5	2.2	
0972JGL00	295.8	298.8	7.3	290.5	5	301.5	9.0	
0973ZEC00	54.4	261.1	−7.1	54.5	1	59.5	6.0	
0974ESL00	334.4	199.7	−6.2	331.5	3	338.5	2.3	
0975SAV00	352.4	210.4	−2.0	352.5	6	344.5	2.0	
0976SON00	169	216.9	−32.6	168.5	1	167.5	6.0	SON0/823FCE0/2.83
0977TCM00	254.6	209.9	−55.5	254.5	3	255.5	12.0	
0978UOE00	209.5	214.2	−49.8	208.5	3	208.5	7.5	
0979ALI00	11.8	208.5	−2.1	4.5	6	18.5	3.0	
0979ALI01	16	204.7	−3.1	4.5	6	28.5	1.8	
0980SEV00	337.9	205.4	6.3	329.5	6	340.5	2.2	SEV0/749NMV0/2.75
0981AGP00	141.1	283.6	37.8	139.5	2907	140.5	22.1	coincides with 007PER, about 20 km/s slower
0982BOC00	76.2	225.0	48.3	60.5	3	76.5	3.0	
0983OCM00	169.6	299.9	−10.6	162.5	3	162.5	12.0	
0984OST00	170.6	268.6	−3.3	167.5	11	165.5	5.3	OST0/896OTA0/2.48
0985TFA00	24.3	303.6	14.9	21.5	4	22.5	30.0	coincides with 827NPE
0986SAD00	194.8	214.6	28.4	196.5	6	197.5	6.0	SAD0/924SAN0/1.07
0987TFC00	218	265.7	−3.8	221.5	10	221.5	2.4	
0988OTC00	214.5	230.4	60.8	214.5	5	216.5	3.0	
0989STH00	350.2	265.3	43.7	351.5	5	350.5	2.4	
0990CHO00	2.2	88.8	−3.7	2.5	0	2.5	0.0	
0991PIC00	52.7	83.1	−2.8	52.5	0	52.5	0.0	
0992GPE00	139.5	282.8	38.2	139.5	2958	139.5	25.7	coincides with 007PER, nearly 30 km/s slower
0993TCP00	178.1	273.2	34.3	178.5	6	179.5	2.7	
0994DBC00	276.6	206.7	−8.6	275.5	12	274.5	5.0	
0995TLS00	68.8	218.2	67.3	60.5	5	64.5	4.0	
0996FMO00	222.2	237.2	−15.6	232.5	10	235.5	1.9	
0997FTP00	139.7	287.3	32.5	140.5	19	122.5	1.3	located about 7° south-west of 007PER
0998ZVD00	287.8	271.4	8.1	288.5	7	287.5	2.5	
0999BEV00	264.7	275.8	−4.8	249.5	6	255.5	1.8	
1000OAM00	206.3	273.8	−29.8	211.5	5	212.5	3.7	
1001UAS00	136.2	194.7	−12.4	148.5	3	147.5	3.0	
1002SVE00	168	239.4	−24.3	162.5	7	161.5	9.0	
1003NAM00	236	246.2	−27.4	238.5	8	242.5	2.7	
1004TFS00	218.5	300.9	−12.2	213.5	4	224.5	6.0	
1005SXO00	190.1	262.5	−2.8	197.5	9	191.5	2.1	
1006ORP00	203.8	288.7	−39.1	203.5	3	204.5	12.0	
1007IVD00	338.7	237.8	8.2	318.5	5	318.5	1.7	
1008LAD00	44.3	243.7	19.4	44.5	2	49.5	4.5	
1009DLD00	320.2	211.9	−5.5	332.5	4	332.5	3.0	
1010LED00	192.1	242.5	−32.7	192.5	3	195.5	3.7	
1011ASD00	2.9	248.3	−3.1	6.5	2	7.5	6.0	
1012ESD00	342.2	245.3	15.2	342.5	5	347.5	2.7	
1013STM00	171.1	295.1	−13.5	183.5	2	161.5	3.0	
1014TNV00	104.6	220.9	43.5	108.5	3	109.5	9.0	
1015TBT00	350.1	201.4	31.9	346.5	3	347.5	12.0	
1016FTS00	78	209.1	4.1	71.5	3	70.5	9.0	
1017AOP00	142.6	210.7	35.5	146.5	3	146.5	9.0	
1018XTC00	160.4	237.1	−5.6	167.5	4	164.5	6.0	
1019MGC00	190.6	242.6	64.3	191.5	4	191.5	2.7	
1020OCI00	198.7	193.5	40.3	207.5	2	206.5	6.0	
1021FOC00	296.2	84.2	−11.2	310.5	1	296.5	0.0	
1022OLA00	191.4	85.0	−1.8	191.5	0	191.5	0.0	
1023NTC00	222.2	91.5	1.4	213.5	1	236.5	3.0	
1024TRP00	241	103.1	26.4	239.5	1	238.5	3.0	
1025CMD00	18.2	165.4	21.0	15.5	4	15.5	7.5	
1026BLE00	174.3	262.9	−44.3	174.5	1	175.5	3.0	
1027OOP00	52.6	208.0	0.1	52.5	7	50.5	3.7	
1028JAV00	288	276.9	−3.4	281.5	5	293.5	2.3	
1029SSU00	117.2	238.2	−35.1	114.5	1	116.5	9.0	
1030FER00	167.8	258.5	−21.2	167.5	22	169.5	4.7	FER0/337NUE0/0.89
1031ZCM00	222.6	257.8	−19.4	236.5	10	237.5	2.5	

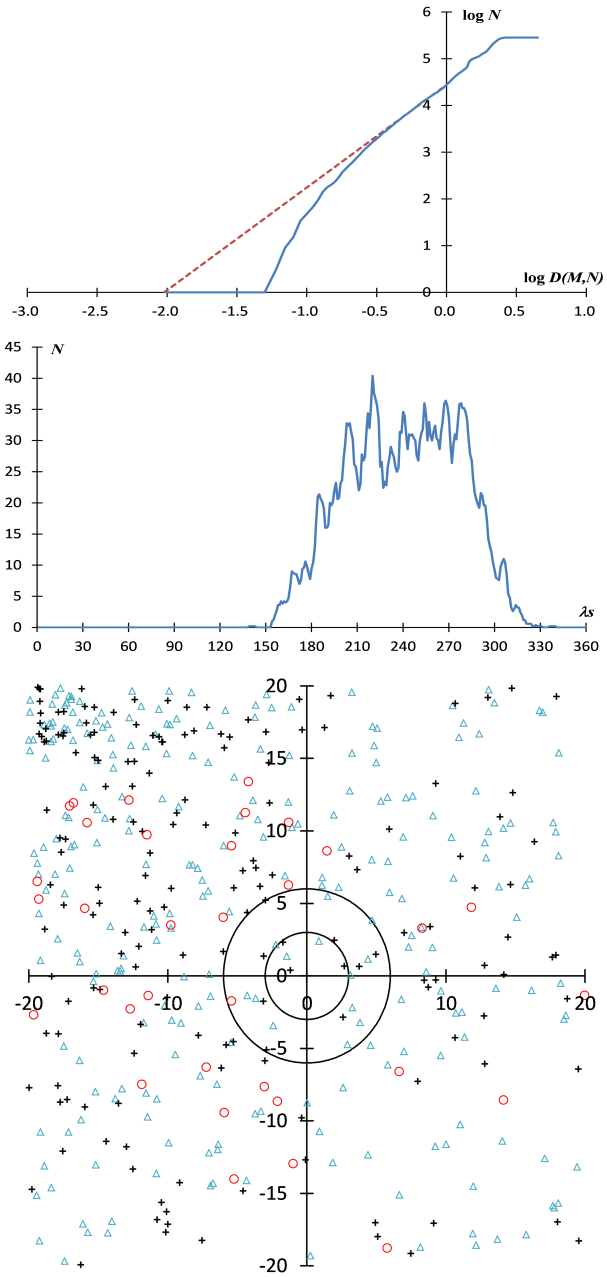

Figure 2 – The shower 0799NEC00.
(a) D_{SH} distribution (top),
(b) number of meteors with $D_{SH} < 0.4$ along with λ_s (middle), and
(c) radiant distributions around the listed $(\lambda - \lambda_s, \beta)$ in Table 1. $D_{SH} < 0.10$: circle, $0.10 < D_{SH} < 0.20$: plus and $0.20 < D_{SH} < 0.40$: triangle.

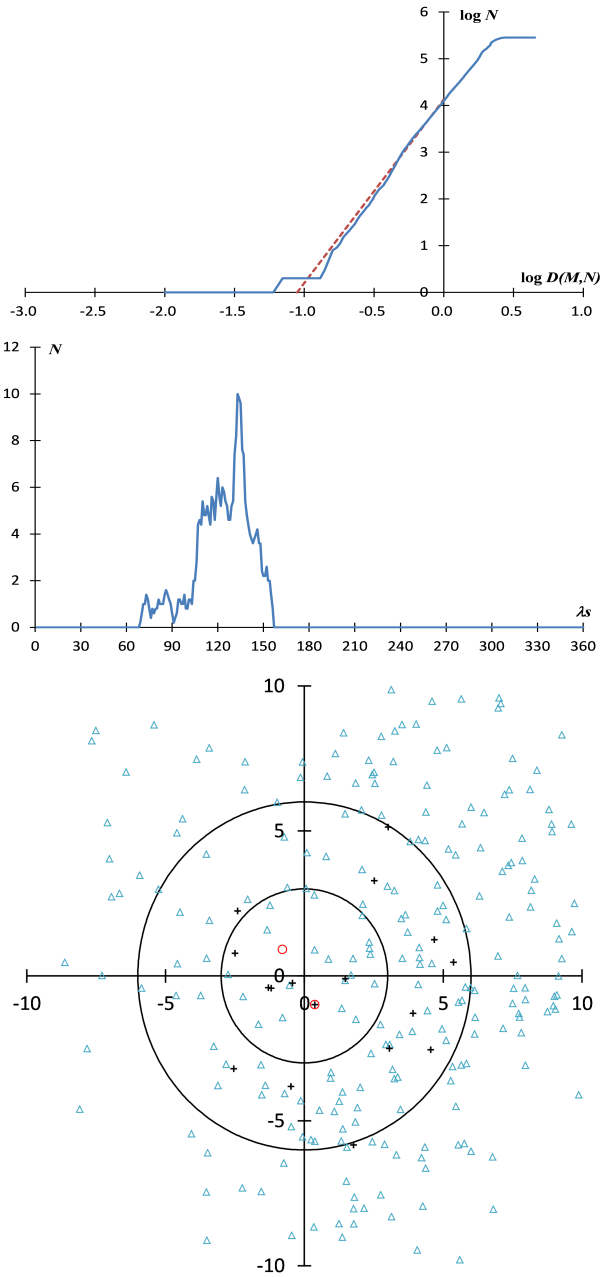

Figure 3 – The shower 0800JCT00. (a)–(c) as explained in Figure 2.

been detected. There are several problems in every search technique whether D based studies or not.

3.1 Problems in OE-based studies

D values are calculated by the four parameters of orbits mentioned in section 1.1: size, form, orientation and crossing angle. We know that meteor shower radiants shift with time and the perihelion orientation moves with time also except for special cases. We calculate D values for the fixed orbit of the maximum and, therefore, such D values for the early and the late activity become larger naturally. It should be stressed ordinary D value based studies give distorted results for the meteor shower active over weeks.

The author showed the estimated orbital elements of the 5 components of the Taurids, taking radiant shift into consideration (Table 4a–e of Koseki, 2020b). We can realize the perihelion of 4 components of the 'Taurids' move with time, i.e., with the solar longitude (λ_s) and, therefore, D values of associated orbits vary with time. SF components (Table 4a of Koseki, 2020b) is the exceptional case having almost stationary perihelion axis. The radiant of the CAP, as we see in Figure 1e and 1f, moves and the axis of the perihelion moves naturally. Figure 1h shows the change of D values for the estimated orbital elements to 0001CAP08 with time (λ_s). If we use the fixed orbital elements to calculate D values, we would miss the early shower members and the late ones as well.

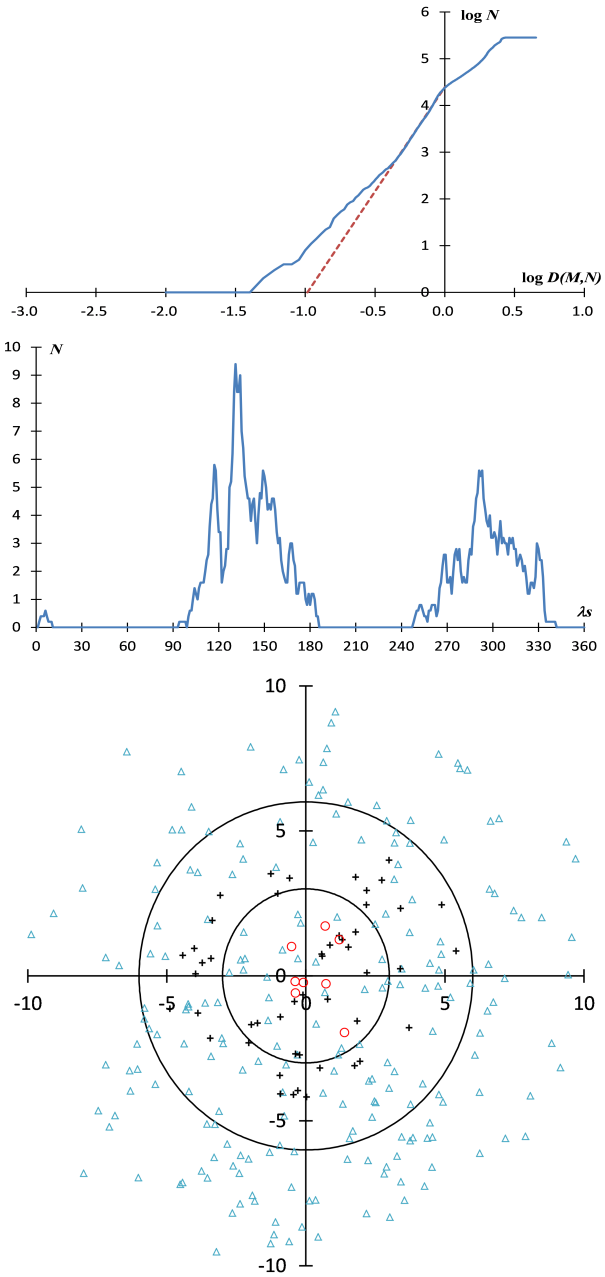

Figure 4 – The shower 0929TXC00. (a)–(c) as explained in Figure 2.

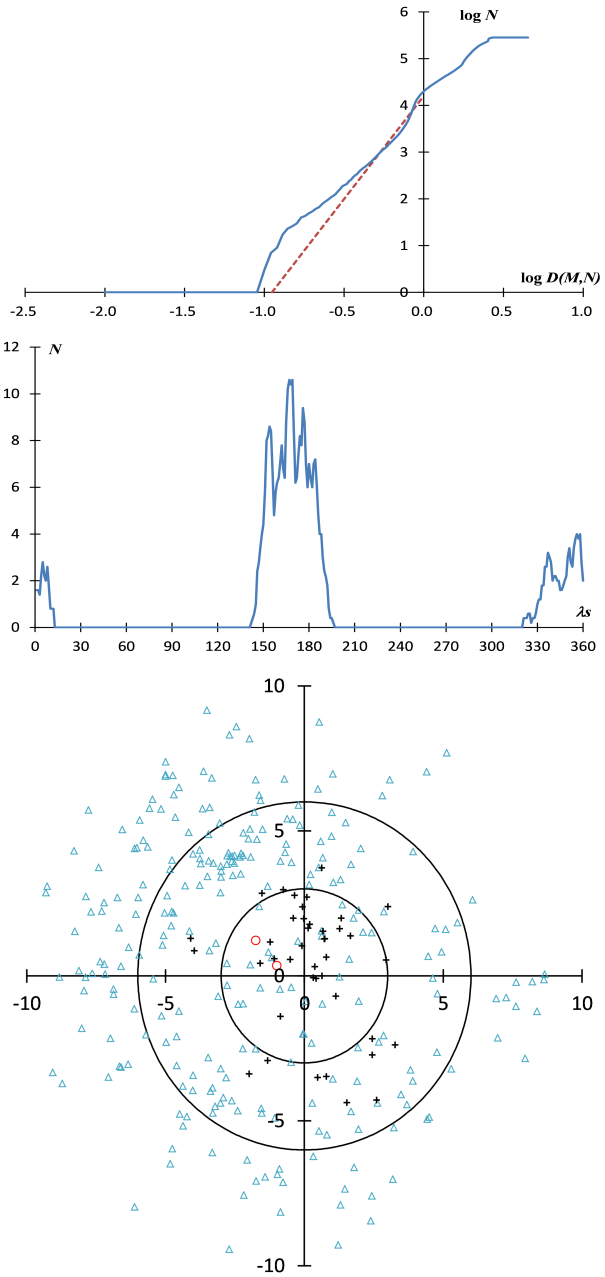

Figure 5 – The shower 1002SVE00. (a)–(c) as explained in Figure 2.

We estimate the sporadic background as the D_{SH} distribution between 0.4 and 1 (Figure 1b for an example) but it seems not proper for Perseids. Figures 6a and 6b compare the difference in the reference D range: Figure 6a for $0.4 < D_{SH} < 1.0$ and 6b for $0.9 < D_{SH} < 1.2$. This peculiarity seems to be caused from the character of Perseid orbit: highly inclined and the length of the activity i.e. the width of the node. It is necessary to pay attention to the D distributions but the range $0.4 < D < 1$ seems to be adequate for finding sporadic background in many showers. Table 2 gives the slope and the intercept of the estimated sporadic background (the dashed line in the figures of the cumulative meteor number). It is clear that the meteor distribution in the four dimensional D value space is quite biased one.

3.2 Problems in radiant based studies

Radiant areas vary widely by the distance from the apex. Radiants with $D_{SH} < 0.1$ of Figure 2c are spread widely but radiants with $0.2 < D_{SH} < 0.4$ are distributed almost within the figure ($r < 10$). It is necessary to note this difference when we search meteor showers with the radiant based study only.

3.3 Problems in BRAMON's research

We find many BRAMON's 'radiants' could not be confirmed by both RP-based and OE-based studies. Their radiants are so sparse that there is no difference from sporadic background in many cases. There might be several problems in addition to ones of OE-based searches.

Table 2 – The difference to the sporadic background distribution. The slope (a) and the intercept (b) of the cumulative D_{SH} distribution. For an example, a and b are the slope and the intercept Figure 1b: 0001CAP08. They are calculated for the range $0.4 < D_{SH} < 1.0$ except for 0007PER04b.

Code	a	b	Remarks
0001CAP08	2.14	4.26	
0004GEM03	0.81	4.70	
0005SDA09	1.49	3.99	
0006LYR03	1.86	3.83	
0007PER04a	0.56	4.45	
0007PER04b	1.87	4.49	$0.9 < D < 1.2$
0008ORI06	1.25	4.58	
0010QUA01	1.51	4.20	
0021AVB04	2.27	4.37	
0031ETA08	1.60	4.04	
0799NEC00	2.20	4.44	
0800JCT00	3.93	4.13	
0801JCD00	7.51	3.91	
0802ADS00	3.22	4.16	
0803LSA00	2.51	4.12	
0804DGR00	3.29	3.56	
0814CVD00	3.32	3.90	
0929TXC00	4.47	4.39	
1002SVE00	4.41	4.20	

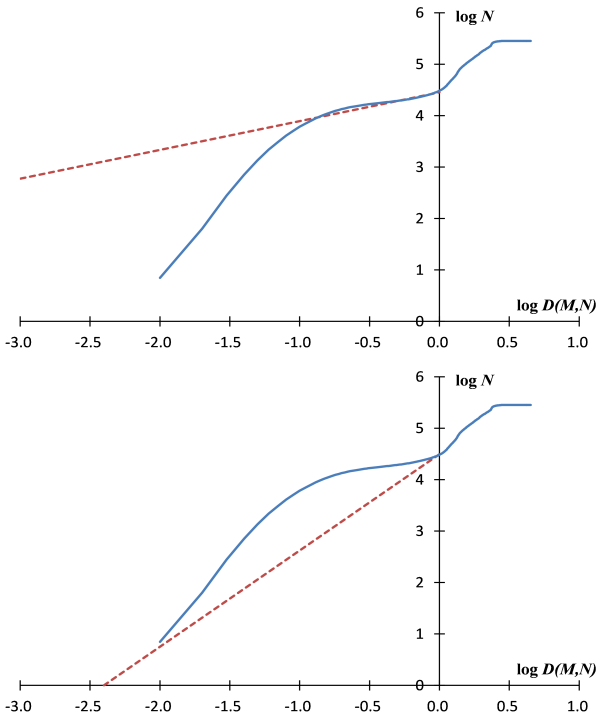

Figure 6 – The difference of the sporadic background in the case of Perseids. (a) using the range of $0.40 < D_{SH} < 1.0$ and (b) using the range of $0.9 < D_{SH} < 1.2$. It is suggested the reference area as sporadic background would be better changed in special cases as Perseids. The author finds $0.40 < D_{SH} < 1.0$ is good enough to estimate sporadic background in many cases.

3.3.1 Data selection

Amaral et al. stated 'not associated with any known radiant should be used' (Amaral et al., 2018). If they removed them according to the identification indicated in the databases, it would not be proper. The authors listed 'probable' meteors as the shower members and excluded 'possible' members which are different from the shower core. Such 'possible' meteors might come from the errors in the observations. A small number of erroneous data might exist in the large amount data though the standard deviations are small enough. Such exclusion may bear some 'new' detections; closely placed from a major shower and weak showers overlapping with a major shower. On the contrary, if the databases include nearby sporadic meteors, the search for meteor showers would be biased.

3.3.2 Cluster analyses

The author used the centroid method of the cluster analysis for compiling meteor shower reference (Koseki, 1986, and also Koseki, 2009) by calculating D_{SH}. There are many techniques in the cluster analysis. It is necessary to be careful with the character of them when applying them. We used the centroid method because the distribution of the meteors/showers might be treated as spherical in the search space.

DBSCAN is often used but one should be careful when selecting the parameters as other clustering techniques require: ε-parameter specifying the radius of a neighbourhood with respect to some point and **minPts** the minimum number of points required forming a dense region. The results depend on what clusters we image and what parameters we select as usual other cluster techniques. It seems very difficult to use DBSCAN for the large amount video data directly. If we divide the data into several smaller groups, it would cause another difficulty; the nature of the groups is different and the recombination of the results should be treated very carefully.

3.3.3 Break point

The break-point method is based on Sekanina's idea (Sekanina, 1970) and it is ideal for the major showers: the number of shower meteors is large enough to define a break point clearly. A 'break-point' might be clearly recognized in theoretical distributions but not so in real meteor distributions. Meteor distribution in the four dimensional space is quite irregular as we saw above (Figures 1b, 2a, 3a, 4a, 5a and Table 2) and, therefore, Sekanina failed in his attempt to detect minor meteor showers. Many meteor showers listed in Harvard-Smithsonian radar survey could not be confirmed as seen in the SD. Amaral et al. (2018) removed 'shower meteors' and the distribution of the remaining meteors might be more distorted. As we studied above, a 'break-point' is recognized barely in BRAMON's showers.

4 Conclusion

Many of BRAMON's new showers include a lot of meteors in the range $0.2 < D_{SH} < 0.4$. Meteors with D_{SH} in this range are usually regarded as being from the sporadic background. It seems reasonable, nevertheless, to confirm the activity of these meteor showers given that they contain enough $D_{SH} < 0.2$ meteors and

that they also show a concentration in RP around a particular center. The author published a paper on meteor shower research using radiant based study (Koseki, 2019) in order to check the SD. The SD has been compiled from meteor showers detected using widely different methods. Searches for 'new' meteor showers should be carried out using two different methods, e.g. OE-based and RP-based studies.

References

Amaral L., Di Pietro C., Trindade L., Zurita M., Silva G., Domingues M., Poltronieri R., Jacques C., and Jung C. (2018). "A search method for meteor radiants". *WGN, Journal of the IMO*, **46:6**, 191–197.

Galligan D. (2001). "Performance of the D-criteria in recovery of meteoroid stream orbits in a radar data set". *MNRAS*, **32**, 623–628.

Koseki M. (1986). "Analysis of meteor data on a microcomputer system". *Journal Brit. Astron. Association*, **95**, 232–240.

Koseki M. (2009). "Meteor shower records: a reference table of observations from previous centuries". *WGN, Journal of the IMO*, **37:5**, 139–160.

Koseki M. (2014). "Various meteor scenes I: the perception and the conception of a 'meteor shower"'. *WGN, Journal of the IMO*, **42:5**, 170–180.

Koseki M. (2019a). "Showers of the IAU Meteor Data Center in the video data of SonotaCo: a simple and clear criterion for grading meteor showers". *WGN, Journal of the IMO*, **47:1**, 7–17.

Koseki M. (2019b). "Profiles of meteor shower activities inferred from the radiant Density Ratios (DR)". *WGN, Journal of the IMO*, **47:6**, 168–179.

Koseki M. (2020a). "Confusions in IAUMDC Meteor Shower Database (SD)". *eMeteorNews*, **5**, 93–111.

Koseki M. (2020b). "Three components of 'Taurids' II". *WGN, Journal of the IMO*, **48:2**, 36–46.

Sekanina Z. (1970). "Statistical model of meteor streams. I. Analysis of the model". *Icarus*, **13**, 459–474.

SonotaCo (2009). "A meteor shower catalog based on video observations in 2007–2008". *WGN, Journal of the IMO*, **37:2**, 55–62. (See also "SonotaCo Network Simultaneously Observed Meteor Data Sets", `http://sonotaco.jp/doc/SNM/`).

Southworth R. and Hawkins G. (1963). "Statistics of meteor streams". *Smithsonian Contr. Astrophys.*, **7**, 261–285.

Handling Editor: Jürgen Rendtel

Radio meteors

Enhanced radio detectability of forward scattered head echoes passing zero Doppler shift

Wolfgang Kaufmann [1]

Object of study was the forward scatter radio observation of sporadic meteors providing a wide spread range of mass, speed and trajectories. A broad distribution of head echo Doppler shifts over the frequency range of the receiving system was anticipated but not found. Instead a noticeable accumulation of head echoes passing zero Doppler shift were observed in a forward scatter setup. An explanation of this phenomenon is pending.

Received 2020 June 19

1 Introduction

First the radio properties of meteors shall be shortly outlined. They were taken from Wislez (2006), Belkovich and Verbeek (2006) and Close et al. (2002). Radio observation of meteors is possible through ionisation of atmospheric gas mainly in heights between 140 down to 70 km (Westman et al., 2004). Two ionised regions have been identified:

1. An approximately spherical sheath of plasma surrounding the meteoroid and moving together with it. Radio reflections from this region are named head echoes. They are subject of strong Doppler shift (up to several ten thousands of Hz at 143 MHz) and are of low power because of the small radar cross section (RCS) of this region. The life time of the plasma sheath starts with the ablation process and is finished when the meteoroid has lost its mass/was decelerated/the ionisation process stopped by growing atmospheric gas pressure. Campbell-Brown and Close (2007) examined the whole lifetime of small meteoroids. They found the ionised phase do not last much longer than 0.5 s. They displayed some ionisation curves of the plasma sheath. These curves represent in principle an optimum function which shapes the power profile, among other things.

2. An approximately conical region of ionised gas of several km of length behind the meteoroid along its trajectory. It is named the trail. Reflections are of high power because of a large radar cross section. They are characterised by the absence of noticeable Doppler shift (some tens of Hz caused by high winds shifting or turbulent parts of the trail). The lifetime of the trail depends mainly on the kinetic energy dissipated in the atmosphere by the meteoroid. A massive ablation creates an intense ionised cone that takes a longer time to become unreflective due to diffusion/recombination processes. In case of an underdense trail the power profile is characterised by a steep rise and an exponential decay. An overdense trail exhibits after the steep rise an elongated phase of reflection with strong power oscillations.

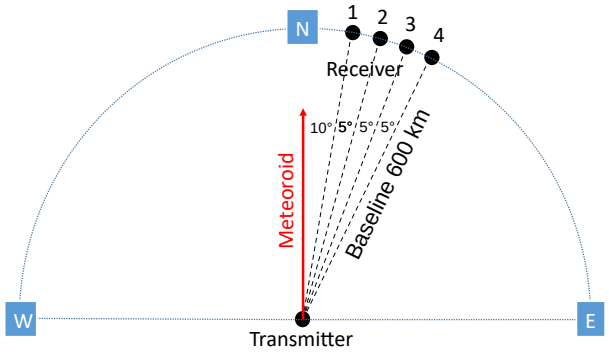

Figure 1 – On top view of the geometry of transmitter, 4 receivers and trajectory of meteoroid.

The forward scatter radio observation of meteor trails is only possible if the geometric arrangement of transmitter, trail and receiving station fulfill the condition of a specular reflection. This is true if the trail is tangent to an ellipsoid with transmitter and receiver as foci. The forward scatter reception of head echoes should be possible at almost all aspect angles due to an approximately isotropically scattering plasma sphere. However it seems to be limited mainly to those head echoes passing zero Hz Doppler shift at the receiving station. It is the aim of this report to analyse this further.

2 Simulation

First a fictive single small meteoroid is investigated during its flight through the atmosphere thereby passing four radio stations. Figure 1 shows a top view on the trajectory of the meteoroid flying straight northward from its starting point in 160 km height directly above the isotropically radiating transmitter. Four receiving station are adopted that have all the same distance from the transmitter but different angles between their baseline and the meteoroid-trajectory. In Figure 2 the Doppler shift curves for these four receiving stations are plotted (speed of the meteoroid is set to 20 km/s, inclination is −15°). Ablation shall start in about 100 km height and shall end at about 96 km (time span = 0.8 s) height as indicated in the graph.

[1]Lindenweg 1e, 31191 Algermissen, Germany.
Email: contact@ars-electromagnetica.de

IMO bibcode WGN-484-kaufmann-detectability
NASA-ADS bibcode 2020JIMO...48..108K

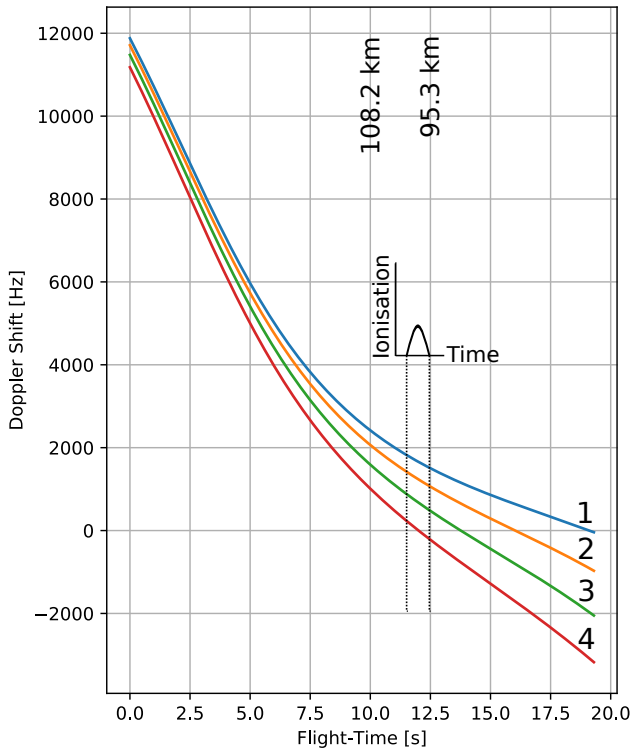

Figure 2 – Doppler shift simulation for the 4 receivers as shown in Figure 1. The indicated ablation phase is picked arbitrarily for demonstration of theoretical considerations.

From Figure 2 we expect head echo reception at the four receiving stations with different Doppler shifted frequencies in the same time period of ablation. The deviation of received power due to different positions of the radio stations is small within this time span: From station 1 to station 4 the decrease in received power is about 15% (calculated on base of the radar equation). Summarised, the same meteoroid produces during its ablation phase at four different stations receivable head echoes with different Doppler shifts and slightly shifted power curves. There is no preference of station 4 where the head echo Doppler shift crosses the zero line.

Generalising we would expect to receive head echoes in a broad Doppler shifted frequency range in form of short duration optimum power curves at an arbitrary radio station. This is strongly supported by the results of a Monte Carlo simulation by German, 2020 (Figure 3). Thereby, the received power will be modulated by the continuously changing transmitter-meteoroid-receiver-distance to a smaller amount and will vary strongly with speed and mass of the meteoroids.

3 Measuring results

Now these assumptions shall be checked against the measured results. Sporadic meteors (SPO) were employed to give a wide spread range of mass, speed and trajectories. Receiving location was Algermissen, Northern Germany. Transmitter was GRAVES-radar in Southern France. In 2018 from January 5 to February 17 continuous head echo monitoring has been performed. Antenna was a HB9CV (theoretical gain 4.2 dbd, no preamp) and the receiver was a software defined radio

Table 1 – Types and proportions of the 34183 meteor signals observed during the 2018 SPO measuring campaign. "off zD" means the meteor signal vanishes before Doppler shift reached zero Hz.

Number of Trail Reflections without Head Echo	Number of Head Echoes without Trail Reflection	Number of Head Echoes with Trail Reflection
29 749	960 + 172 off zD	3 301

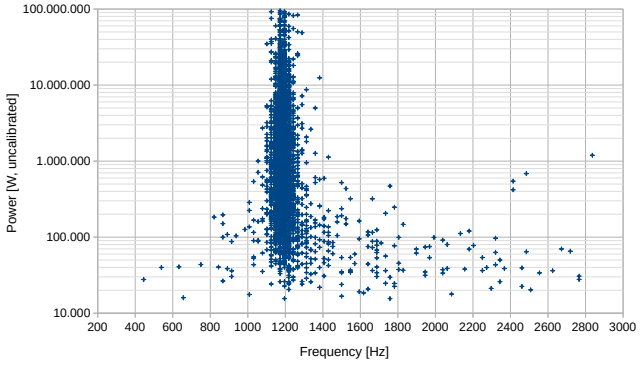

Figure 3 – Received power maximum per head echo versus the associated frequency in a 6 week monitoring session 2018, Jan-Feb. in Algermissen, Northern Germany (4434 head echoes). The measured power is not calibrated.

FUNcube Dongle Pro+[a] running with SDR#[b]. This means all signal processing from digitised radio frequency to demodulated audio frequency is implemented by mathematical algorithms. Especially frequency filtering do not suffer from curved passband characteristics. Recording software was MeteorLogger[c] (Kaufmann, 2017). The USB-demodulation of the unshifted cw signal of GRAVES-radar denotes at 1195.3 Hz.

Head echoes with and without an associated trail reflection and also trail reflections without a head echo were found, proportions see Table 1. These types of meteor signals also are described by Zhou et al., 1998. The identification of head echoes was performed by means of

[a] http://www.funcubedongle.com
[b] https://airspy.com
[c] http://www.ars-electromagnetica.de/robs/download.html

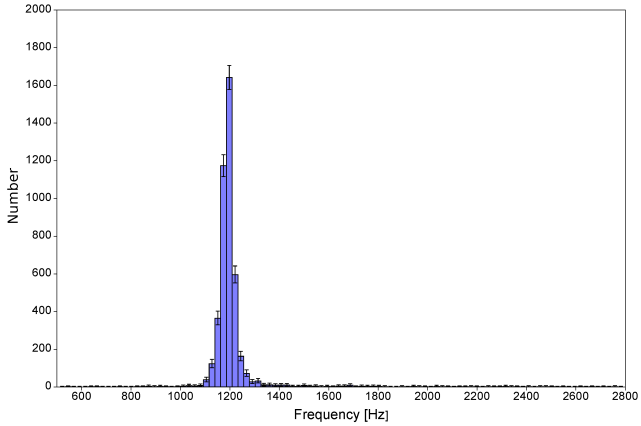

Figure 4 – Frequency distribution of the 4434 head echo frequencies at maximum power from Figure 3.

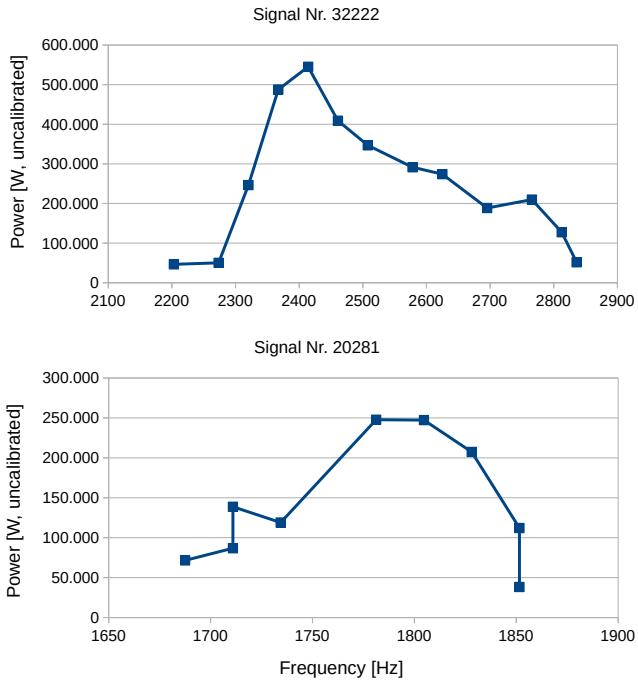

Figure 5 – Examples of received power curves of two head echoes off zero Hz Doppler shift (= 1195.3 Hz), taken from the underlying data set of Figure 3.

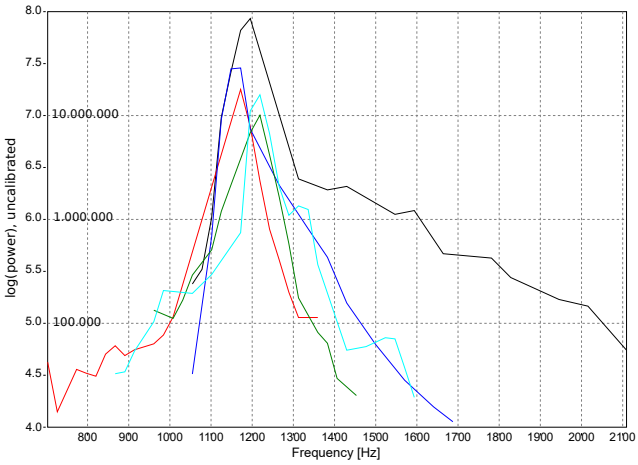

Figure 6 – Examples of received power curves of five head echoes near zero Hz Doppler shift (= 1195.3 Hz) without masking trail reflection, taken from the underlying data set of Figure 3.

a python script (experimental version 1.69 of ProcessData, it is available on request from the author) which traces the head echoes from their first emergence until they vanish or get superimposed by the more powerful trail reflection. Thereby a head echo signal must last at least 50 ms and must show a frequency decline of at least 70 Hz to be counted as head echo (criteria were empirically determined to exclude false positives from rf-noise). Superimposition by the trail reflection causes some under-representation of head echo signals in the frequency range below zero Doppler shift (1195.3 Hz).

Figure 3 shows the received power maximum per head echo versus the associated frequency. Figure 4 displays these data as histogram. Contrary to the expectation, there is no broad spread pattern of received head echo power curves with different power levels and Doppler shifts. Instead, head echo power curves show to be most powerful and hence most numerous near zero Hz Doppler shift. With increasing Doppler shift we find a rapidly decreasing number of head echoes with rapidly decreasing power levels. Figures 5 and 6 show examples of power curves of meteoroids off and at about zero Hz Doppler shift, respectively. Note the different power scaling between the Figures. Figure 7 depicts the distribution of the duration of all recorded head echoes. The dominance of short termed head echoes accounts for prevailing smaller meteoroids. Also the modest sensitivity of the receiving equipment in use and the large distance to the southward directed main beams of GRAVES radar contribute to the observed overall short duration.

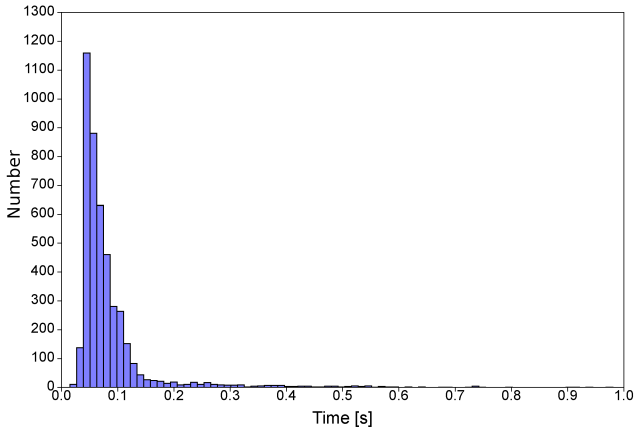

Figure 7 – Distribution of the duration of 4434 recorded head echoes from Figure 3.

4 Discussion

We found the anticipated head echo power curves spread over the receiving frequency range. However, their power maxima and their occurrence are not randomly distributed over the frequency receiving range. The overwhelming number of observed head echo power curves culminate near zero Hz Doppler shift. Their power maxima are by many orders of magnitude larger than the power maxima of head echo power curves received at frequencies off zero Hz Doppler shift. It appears that head echoes reaching zero Doppler shift during the ablation process of the meteoroid have a significantly enhanced chance of reception in a forward scatter set up. Consequently, only the less numerous larger meteoroids with higher RCS could be detected off zero Hz Doppler shift.

At the point where the meteoroid's trajectory is tangent to an ellipsoid with TX and RX as focal points not only a section of the trail becomes reflective towards the receiver but also the Doppler shift of the head echo becomes zero (Verbelen, 2019). From Mathews et al. (2010) the existence of head-trail interference is known. Maybe constructive interference can be an explanatory approach to the enhanced observation of zero Doppler shift passing head echoes.

Besides this unexplained effect two further questions arise from Table 1:

1. There is a small number (960) of head echoes reaching zero Doppler shift without a trail: The ablating meteoroid is tangent to the TX-RX-ellipsoid at the moment the head echo Doppler shift becomes zero. Consequently its ionised trail must also become tangent to the ellipsoid. The trail fulfills the specular condition at this point and a trail reflection should be receivable. The observed aberration may be explained by high gusty winds moving the trail out of the specular condition shortly after its formation.

2. There is an overwhelming number (29749) of trail reflections without head echo: The existence of a trail reflection claims the existence of a meteoroid with a co-moving plasma sheath and a trajectory tangent to the TX-RX-ellipsoid. Therefore, a head echo should be present. This phenomenon may be explained by the mass distribution of the meteoroids. Most are very small and therefore having very small RCS contrary to their trails. Especially when the reflection do not happen in the main beam of GRAVES radar but is produced in its low power side lobes only the head echoes of the much less number of large meteoroids can be detected with the simple radio equipment in use. Also, as described above, a criterion for identification of a head echo was a duration of at least 50 ms. Therefore, all very short termed weak head echoes remained undetected.

5 Conclusion

In this study the detectability of head echoes in a forward scatter setup was found to be significantly increased if their Doppler shift passes zero. This leads to a seemingly concentration of head echoes with zero crossing Doppler shifts whereas the number of observable head echoes never passing zero Doppler shift is comparatively very small. This enhancing effect enables the amateur to receive a substantial number of head echoes with a simple radio equipment compared to professional radar meteor observation stations. The author would like to encourage radio meteor observers to examine their data whether the above described phenomenon is of general validity. May be a meteor scientist is willing to identify the underlying mechanism.

Acknowledgement

The author thanks Mike German and Hans Wilschut for many helpful discussions and valuable input and Jeans-Louis Rault for reviewing the draft and giving important advice and encouragement.

References

Belkovich O. J. and Verbeek C. (2006). "The physics of meteoroid ablation and the formation of ionized meteor trails". In Verbeeck C. and Wislez J.-M., editors, *Proceedings of the Radio Meteor School 2005*. IMO, pages 21–26.

Campbell-Brown M. D. and Close S. (2007). "Meteoroid structure from radar head echoes". *Mon. Not. R. Astron. Soc.*, **382**, 1309–1316.

Close S., Oppenheim M., Hunt S., and Dyrud L. (2002). "Scattering characteristics of high resolution meteor head echoes detected at multiple frequencies". *J. Geophys. Res.*, **107 (A10)**, 1295.

German M. T. (2020). "A head echo Doppler model for assessment of meteoroid forward scatter characteristics". *WGN, Journal of the IMO*, **48:1**, 4–11.

Kaufmann W. (2017). "New radio meteor detecting and logging software". *WGN, Journal of the IMO*, **45:4**, 67–72.

Mathews J. D., Briczinski S. J., Malhotra A., and Cross J. (2010). "Extensive meteoroid fragmentation in V/UHF radar meteor observations at Arecibo Observatory". *Geophys. Res. Letters*, **37**, L04103.

Verbelen F. (2019). "Meteor velocity drived from head echoes obtained by a single observer using forward scatter from a low powered beacon". *WGN, Journal of the IMO*, **47:2**, 49–54.

Westman A., Wannberg G., and Pellinen-Wannberg A. (2004). "Meteor head echo altitude distributions and the height cutoff effect studied with the EISCAT HPLA UHF and VHF radars". *Annales Geophysicae*, **22:5**, 1575–1584.

Wislez J.-M. (2006). "Meteor astronomy using a forward scatter set-up". In Verbeeck C. and Wislez J.-M., editors, *Proceedings of the Radio Meteor School 2005*. IMO, pages 85–107.

Zhou Q. H., Perillat P., Cho J. Y. N., and Mathews J. D. (1998). "Simultaneous meteor echo observations by large-aperture VHF and UHF radars". *Radio Science*, **33**, 1641–1654.

Handling Editor: Jean-Louis Rault

Frequency shifts of head echoes in meteoroid trail formation

Hans W. Wilschut [1]

The approximate frequency shift of a radar echo from a meteoroid is derived. The origin of head echoes are discussed by considering schematic models.

Received 2020 June 29

1 Introduction

Many aspects concerning radio echoes from meteoroid trails can be understood in terms of the line-oscillator model. The standard work for this is McKinley's book (McKinley, 1961), chapters 8 and 9. However, McKinley does not show how frequency shifts near the optimal reflection point can be calculated. In this paper the formalism of (McKinley, 1961) is extended to include frequency shifts. In doing so a close relation appears between the line-oscillator and what is referred to as the "moving ball" model. In the latter model frequency shifts occur because the radio echo will be Doppler shifted.

Inspecting measured meteoroid radio echo's such as shown in Figures 2 and 3 one can observe two distinct parts. The first part is a signal with a frequency deviating from the transmitter frequency and the second part, which extends over longer time, is centered around the transmitter frequency. This first part is often referred to as the "head echo". Many authors interpret this signal in terms of Doppler shifts. The larger second part is well understood as a reflection from the trail left behind after a meteoroid passed. The free thermalized electrons in the trail can cause strong reflections of the radio signal when their individual amplitudes add coherently. The head echo is produced during trail formation. In the line-oscillator description the scattering electrons, created as the trail is formed, will have relative phases such that it appears as a frequency shift away from the emitter frequency. This is not the Doppler shift due to reflections on a co-moving plasma. The latter is assumed in the moving ball description. Some recent work on Doppler shifts in head echoes can be found in this journal. See for example (Kaufmann, 2020; Verbelen, 2019; German, 2020).

One aim of this paper is to derive an approximate value of the frequency shift using the line-oscillator model of (McKinley, 1961). The notation of that work will be followed unless otherwise indicated. For the convenience of the reader some of the formalism in McKinley (1961) will be repeated here. The derivation of the frequency shift in this model will be given in the next Section. The third Section considers the case of Doppler shifts, showing the close connection with the line-oscillator model. In Section 4 examples of calculations are made for a qualitative comparison with observations. Section 5 gives a suggestion why spectra like the one shown in Figure 2 with only a half head echo are seen more frequently than the one in Figure 3 with a complete head echo. The final section contains some concluding remarks.

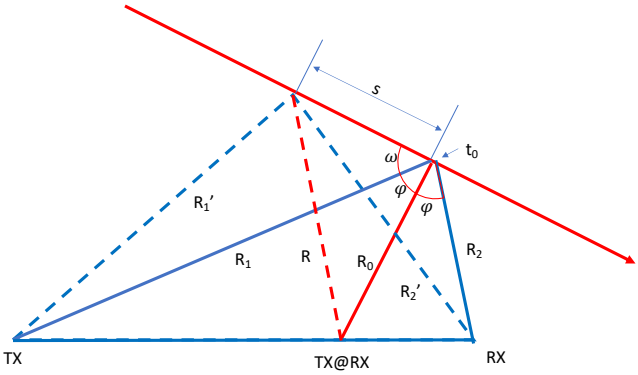

Figure 1 – [Color on-line] TX and RX are the locations of the transmitter and receiver, respectively. The signal path for back scattering (red) and for forward scattering (blue) is shown for the optimal path corresponding to the reflection (specular) point, t_0, (full lines) and the path of a contributing neighboring point (dashed lines) separated by a distance s.

2 Derivation of the frequency shift

When an ionized trail is made by a meteoroid (see Figure 1), the created free electrons act as individual scatterers, they re-emit the signal of a transmitter in all directions. These can be observed in a receiver contributing an amplitude dA_R

$$dA_R \propto \sin\left(2\pi f t - \frac{2\pi(R_1' + R_2')}{\lambda}\right) , \qquad (1)$$

where λ is the transmitters wavelength and f its frequency. (All other parameters in this work are defined in Figure 1.) Each scattering contribution has a different phase depending on the distance $(R_1' + R_2')$ the signal travels. Going along the trail the addition becomes coherent when $d(R_1' + R_2')/dt = 0$. At this point the path followed is a reflection, the specular condition. The length of this path is $R_1 + R_2$ and is the shortest path between transmitter and receiver via a point on the meteoroid trajectory. This point will be referred to as the specular point. Figure 1 also shows signal paths corresponding to back scattering. This is the radar setup, where emitter and transmitter are at nearly the same location. An arbitrary path has length $2R$ and the shortest path is $2R_0$. Near the specular

[1]Van Swinderen Institute, University of Groningen.
Email: hwwilschut@gmail.com,
Permanent address: Sankt Augustin, Germany.

IMO bibcode WGN-484-wilschut-shifts
NASA-ADS bibcode 2020JIMO...48..112W

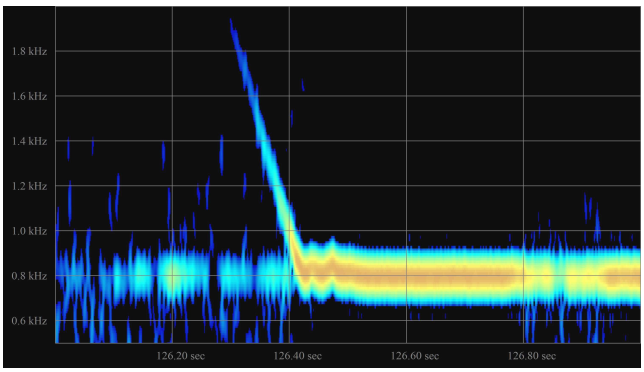

Figure 2 – [Color on-line]Typical example, of a strong head echo. The horizontal scale is one second long, the vertical scale 1.5 kHz. The slope corresponds to −9.7 kHz/s Data were taken 05 May 2020 in Kampenhout (BE) using the 49990 kHz VVS beacon near Ieper (BE) (F. Verbelen, private communication).

.

point where $s \ll R_0$ one finds that

$$\begin{aligned} &R_1' + R_2' \approx \\ &\approx R_1 + R_2 + \frac{s^2 \sin^2\omega}{2}\left(\frac{1}{R_1 - s\cos\omega} + \frac{1}{R_2 + s\cos\omega}\right) \\ &\approx R_1 + R_2 + \frac{s^2 \sin^2\omega}{2}\ \frac{R_1 + R_2}{R_1 R_2}\ . \end{aligned} \tag{2}$$

This reduces to

$$R \approx R_0 + \frac{s^2}{2R_0} \tag{3}$$

for back scattering. Also note that in chapter 9 of (McKinley, 1961) the notation was changed: $s \rightarrow f$ or f. Here we will use s consistently for the path of the meteoroid. Further note that, in general, $\omega \neq \pi/2 - \phi$ because the trail may make an angle β with the plane where forward scattering takes places, in which case $\sin^2\omega = 1 - \sin^2\phi\cos^2\beta$.

Central to the problem is the summation over individual scatterers along the trail. The model assumes a constant ionization density along the trail, the amplitude is then given by

$$A_R \propto \int_{x_1}^{x} \sin(\chi - \frac{\pi x^2}{2})dx\ . \tag{4}$$

Following (McKinley, 1961), we first evaluate the integral for back scattering where $2s = x(R_0\lambda)^{1/2}$ and $\chi = 2\pi ft +$ a time independent phase. Thus one sums from the beginning of the trail until a point $s(t)$, i.e. the length of the trail at time t. Without loss of generality $x_1 \rightarrow -\infty$ can be assumed, as shown explicitly in Section 4. One obtains

$$A_R \propto \left(C(x) + \frac{1}{2}\right)\sin\chi - \left(S(x) + \frac{1}{2}\right)\cos\chi\ , \tag{5}$$

where C and S denote Fresnel integrals[a]. To see what this means for the frequency we look at times $t < t_0$ and $t > t_0$ avoiding the complex behavior near t_0 by considering $|x| \gtrapprox 1$. With this approximation

$$\begin{aligned} A_< &\propto \frac{\cos(\chi - \frac{\pi x^2}{2})}{\pi x} \text{ and} \\ A_> &\propto \sin(\chi) - \cos(\chi) + \frac{\cos(\chi - \frac{\pi x^2}{2})}{\pi x}\ . \end{aligned} \tag{6}$$

As t approaches t_0 the amplitude $A_<$ increases slowly compared with the frequency f. At each t the instantaneous frequency f_i can be obtained by determining the phase Φ of $A_<(t)$

$$\Phi = \chi - \frac{\pi x^2}{2} = 2\pi ft - 2\pi\frac{s^2}{R_0\lambda} \tag{7}$$

and taking its derivative with respect to t, giving

$$f_i = \frac{1}{2\pi}\frac{d\Phi}{dt} = f - \frac{2s\ ds/dt}{R_0\lambda}\ . \tag{8}$$

Note that here $s > 0$ and $ds/dt < 0$, the shift is thus positive. In practice one analyses the change in the instantaneous frequency f_i,

$$\frac{df_i}{dt} = -2\left(\left[\frac{ds}{dt}\right]^2 + s\frac{d^2s}{dt^2}\right)\frac{1}{R_0\lambda}\ . \tag{9}$$

A simple model choice is a constant velocity where $s = |V(t_0 - t)|$, so that

$$\frac{df_i}{dt} = -\frac{2V^2}{R_0\lambda}\ . \tag{10}$$

To obtain the shift in forward scattering one simply replaces Equation 3 with Equation 2 to find

$$\frac{df_i}{dt} \approx -\frac{V^2\sin^2\omega}{\lambda}\frac{R_1 + R_2}{R_1 R_2}\ . \tag{11}$$

For $t > t_0$ there is no such simple derivation for the phase of $A_>$ possible. In order to get insight numerical calculations were done. These will be discussed in Section 4.

3 Derivation of the frequency shift in terms of Doppler shifts

In this section we consider the possibility that only a short part of the trail survives, so that it has a length $x < 1$. Thus where at the front free electrons are created they disappear at the back. Therefore, the trail has a constant length Δx. In fact for the observer it appears as a passing object, which maybe as well be the meteoroid itself. When this object passes point t_0 it will give an echo. In this case one can approximate Equation 4 by

$$A_R \propto \sin(\chi - \frac{\pi x^2}{2})\Delta x\ . \tag{12}$$

The phase of this amplitude is identical to that in Equation 7 and the same relations hold for the shifts. The shift continues for $t > 0$ where the instantaneous frequency, f_i, is lower than the emitter frequency f.

[a]Here $S(z) = \int_0^z \sin\frac{\pi t^2}{2}dt$ and $C(z) = \int_0^z \cos\frac{\pi t^2}{2}dt$

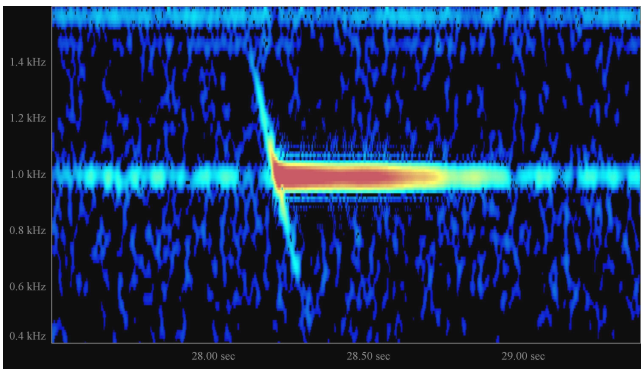

Figure 3 – [Color on-line] Less common head echo showing a shift that extends to negative shifts. The slope is −4.9 kHz/s. Data taken on 09 June 2011 in Kampenhout using the 49970 kHz BRAMS beacon at Dourbes (BE)(F. Verbelen, private communication).

.

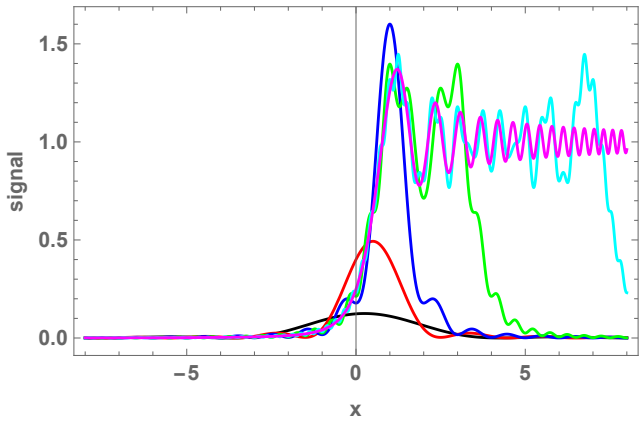

Figure 4 – [Color on-line] $\overline{A_R^2(x(t))}$ for $\Delta x = 0.5, 1, 2, 4, 8, \infty$ (black, red, blue, green, cyan, magenta).

The bistatic Doppler shift is given by $-\frac{1}{\lambda}d(R_1' + R_2')/dt$. Using the same approximations as Equation 2 one arrives at the identical expression as in Equation 8. Thus the shifts are the same as they must be, because of Galilean invariance. A more informative evaluation will come from a numerical calculation in the next section. The main conclusion of this section is, that it will be very difficult for the amateur observer to differentiate between the meteor as a moving object and it forming a trail.

If one insists on interpreting the formalism discussed in this section as a meteoroid model one has to consider typical parameters. For the observations in Figures 2 and 3, assuming an underdense trail, the value of the ambipolar diffusion time is of the same order as the passing of half a Fresnel length (20 ms), it does not allow a sharp boundary on the trail. On the other hand, assuming an overdense trail, the meteoroid appears as an object with a metallic surface with a much sharper boundary and with a size smaller than a wavelength (Pellinen-Wannberg, 2005) (see also Section 5).

4 Example Calculations

At this point it may be interesting to consider in more detail how the signal appears on observation. The result of Sections 2 and 3 can be generalized into one expression

$$A_R \propto \big(C(x) - C(x-\Delta x)\big)\sin\chi - \big(S(x) - S(x-\Delta x)\big)\cos\chi\ , \tag{13}$$

where Δx is the length of the object or trail as defined above. In the following calculation we use for s the backscatter configuration with $V = 30$ km/s, $R_0 = 100$ km, and an emitter frequency $f = 50$ MHz.

First we consider the signal power, $\overline{A_R^2(t)}$, which is obtained by averaging over a time long with respect to the frequency but small with respect to $x(t)$. In Figure 4 this quantity is shown, evaluated for various values of Δx. For small Δx the signal has a nearly Gaussian dependence, where it should be noted that $x = 1$ corresponds to about one Fresnel zone (here it corresponds to $t = \sqrt{\lambda R_0}/2V = 13$ ms or a distance of 387 m). At this small distance the signal has the characteristics of Fraunhofer slit scattering. For $\Delta x > 2$ and $x > 1$ one observes what are called Fresnel oscillations. $\Delta x = \infty$ refers to the situation discussed in Section 2; the pattern seen here corresponds to Fresnel edge scattering. The oscillation frequency in the Fresnel pattern (see chapter 8, eq. (8-15) in (McKinley, 1961)) is identical to the frequency shift calculated in Section 2. In fact, historically, it has been a main tool for determining meteoroid velocities instead of the frequency shift.

To observe the frequency dependence of Equation 13, it should be displayed as a time dependent frequency spectrum similar to the observed data. This can be done by a Short Time Fourier Transform (STFT) of the theoretical expressions for A_R in Equation 13 (see Appendix 6). The results are shown in Figure 5. First we discuss the spectrum (top) which is close to what was discussed in the previous section. The size of the object or trail passing through the specular point is taken to be $\Delta x = 1$. The signal has the characteristic Doppler shift dependence with a maximal amplitude at the specular point. Superimposed is a Fraunhofer diffraction spectrum. This pattern has to occur independent of the interpretation of the object in terms of a a short-lived trail or as moving object. The spectrum on the right is for $\Delta x = \infty$, the line oscillator model of Section 2. It is dominated by the ridge at $f_i - f = 0$ at $t > t_0$. Its origin is the stationary trail. The diagonal in the spectrum has the same time-frequency dependence as the left-hand spectrum but without the diffraction pattern. This is the head echo from the trail as it is being formed.

There are several observations to be made at this point: The Fresnel oscillations found in Figure 4 are not seen in the spectrum. They appear by reducing the Hann window in the STFT (see Appendix 6). Calculations were made for a window width of 0.5, 1 and 2 Fresnel zones. For the short window the oscillations can be seen, but at the cost of resolution in frequency. This is characteristic for a Fourier transform where time and frequency resolution exclude each other mutually. In Figure 6 the frequency spectrum is shown at $t = 0.2$ s for the three Hann windows. The spectrum with the

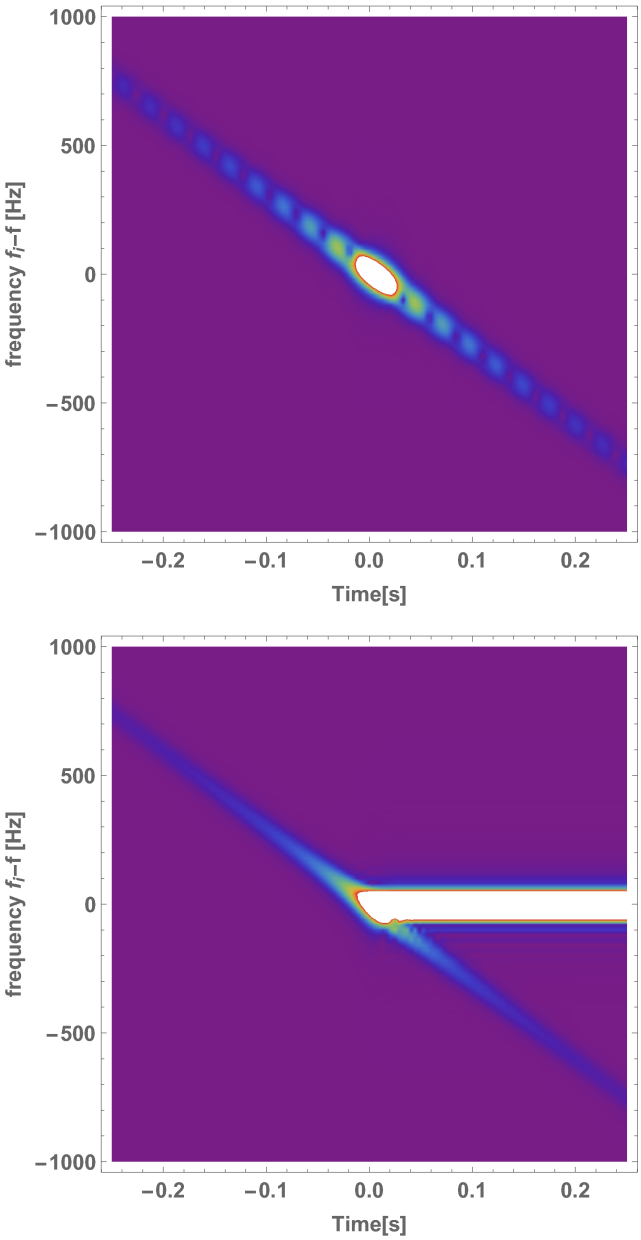

Figure 5 – [Color on-line] Time versus frequency of $\log(A_R)$ obtained with a STFT procedure. Top: passing trail or object. Bottom: Dynamic meteoroid trail. See text.

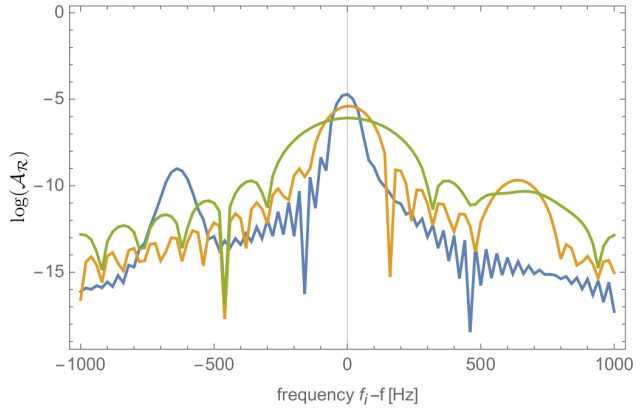

Figure 6 – [Color online] Frequency spectrum of $\log(\mathcal{A}_\mathcal{R})$ at $t = 0.2$ s the green, orange and blue curves refer to an average over 0.5, 1, and 2 Fresnel zones, respectively. The branch of the head echo is at −700 Hz. See also text.

largest Hann window was also used to obtain Figure 5. The branch of the head echo is clearly seen for that window, while for the smallest window it has all but disappeared due to the reduced frequency resolution. Notice that the head echo signal is more than 100 times smaller compared to the signal of the stationary trail. This indicates that measuring the head echo at $t > t_0$ requires that the receiver settings and the associated analysis programs need to take the time average in consideration. The observation of the frequency shift at $t < t_0$ is rather robust and thus also in an actual measurement. If possible, one could determine both the Fresnel oscillations and the frequency shift by analyzing the data in two different ways by good time and poor frequency resolution and vice versa, respectively. In this way one has two ways to measure the meteoroid velocity.

One might expect measured events as in Figure 3 to be the most common. However, most observations are as in Figure 2. This is either due to problems associated with measuring the head echo at $t > t_0$ for the reasons mentioned above or because the line-scattering model is not describing the meteoroid events adequately. Another reason for this can be the observational bias for strong echoes with a short trail below the specular point.

5 The half-ball model

The characteristic asymmetric behavior of the head echo noticed at the end of the previous section can be resolved assuming reflections from the plasma in front of – and moving with – the meteoroid. Research around 2000, for example with Arecibo (Mathews et al., 1997), ALTAIR (Suggs et al., 1994) and more recently in EISCAT (Pellinen-Wannberg, 2005; Kero et al., 2008) shows the importance of the head echo plasma. Such a plasma reflects radio waves like a metal mirror. The specular condition is then irrelevant since there will always be a spot on a sphere allowing reflection from transmitter to receiver; also, in forward scattering. But in forward scattering it is important to realize that only the front half of the meteoroid has this property. The situation is sketched in Figure 7. Only in the approaching phase reflections are possible up to the specular point, after that reflections would have to come from the back of the meteoroid. Therefore, in this scenario a true Doppler shift signal is observed until $t = t_0$, and after that only the trail left by the meteoroid at the specular point contributes to the signal. This scenario, which could be called the "half-ball model", would explain experimental data as in Figure 2.

Reflections at the specular point proceed via the shortest path between transmitter and receiver and therefore also give the strongest reflection in this model, as it does in the line-oscillator model. It will be interesting to combine line-oscillator model (observing the back tail) with the "half-ball model" as the relevant trail parts do not pass the specular point at exactly the same time. In any case it is somewhat surprising that the head plasma reflection is strong enough to be seen in a comparatively modest amateur setup. The difference

with an extensive High-Power Large-Aperture setup is striking, in the EISCAT configuration the asymmetry between positive and negative Doppler shifts is not observed (Kero et al., 2008). The observational bias of these setups is, of course, large and less powerful setups will see only a subset. Most amateur reporting concerns the number of observations or determining the frequency shift. It will be interesting to also quantify which patterns are observed (e.g. Figure 2 vs. 3) and, in this way, get better insight of what is observed.

6 Conclusions

Two very different approaches lead to the same shifts in the radio-echo frequency when a meteoroid passes through a point where the specular condition is fulfilled. One assumes either thermalized electrons in the local atmosphere or electrons co-moving with the meteoroid as the scatterers. They lead to the same frequency shifts because they are both based on the time derivative of Equation 2. The model discussed in Section 2 describes head echoes and the resulting stationary trail in a unified way. More explicitly, further calculations in Section 4 show that frequency shift and the Fresnel diffraction pattern relates to the same observable (Equation 8). In Section 3 it was shown that a short-lived trail and a moving object give the same frequency shift of the head echo as in Section 2. The size of the object must have $|x| \lessapprox 1$, i.e. one Fresnel zone. The calculations show that in these cases a diffraction pattern should be visible on the head echo. In practice this is not observed. This may be because of the simplicity of the model. The calculations in Section 4 allow for a qualitative comparison with actual observations. The contradicting requirements for frequency and time resolution were pointed out and it was also shown that this is reflected in the duality observing either the Fresnel diffraction or the frequency shifts. This duality may also play a role in the absence of a head echo at $t > 0$ in most observations. Another reason for this can be the observational bias for strong echoes with a short trail below the specular point. However, assuming that a co-moving plasma in front of the meteoroid is important, there is a simple geometric argument why there is no head echo after the meteoroid passes the specular point t_0.

As a final remark and recommendation: The measurements of meteoroid echoes contain much more information than the frequency shifts. In particular more detail about the Doppler shift distribution around the emitter frequency may provide hints as to the precise nature of a meteoroid event. Modern equipment available to the amateur, allows a quantitative measurement of the signal strength and frequency distribution; the classic text of (McKinley, 1961) provides several methods for its analysis.

Acknowledgement

The author thanks F. Verbelen, W. Kaufmann, and M. T. German for clarifying some of the concepts in radio meteoroid measurements, for sharing their data, and for discussions.

References

German M. T. (2020). "A head echo Doppler model for assessment of meteoroid forward scatter characteristics". *WGN, Journal of the IMO*, **48:1**, 4–11.

Kaufmann W. (2020). "Limitations of the observability of radio meteor head echoes in a forward scatter setup". *WGN, Journal of the IMO*, **48:1**, 12–16.

Kero J., Szasz C., Wannberg G., Pellinen-Wannberg A., and Westman A. (2008). "On the meteoric head echo radar cross section angular dependence". *Geophys. Res. Lett.*, **35:7**, L07101.

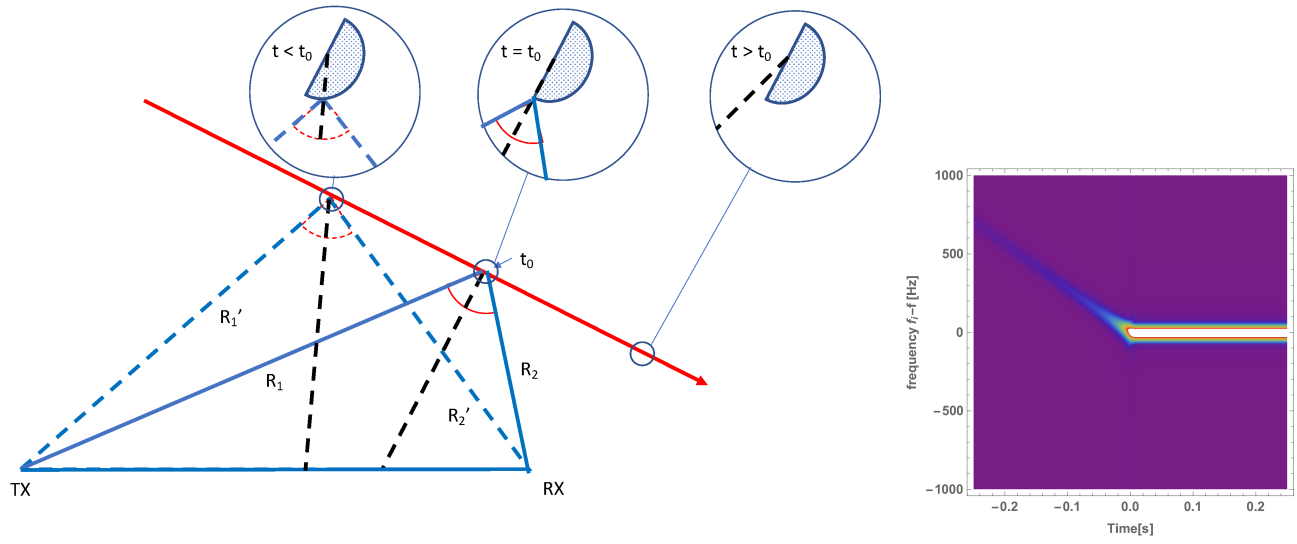

Figure 7 – [Color on-line] Half-ball model. An echo can be seen at any point along the meteoroid trajectory. But only from the front plasma of the meteoroid. After passing the specular point ($t = t_0$), there will be no echo any longer except from the stationary trail. The right hand side shows a calculation where this was implemented in the line-oscillator model although this is not the right model for such a scenario.

Mathews J. D., Meisel D. D., Hunter K. P., Getman V. S., and Zhou Q. (1997). "Very High Resolution Studies of Micrometeors Using the Arecibo 430 MHz Radar". *Icarus*, **126:1**, 157–169.

McKinley D. W. R. (1961). *Meteor Science and Engineering*. McGraw-Hill, New York.

Pellinen-Wannberg A. (2005). "Meteor head echoes - observations and models". *Annales Geophysicae*, **23:1**, 201–205.

Suggs R. M., Cooke W., Brown P., Coster A., Close S., Hunt S., and Durant D. F. (1994). "Meteor properties dara base – final report". *Technical report SEE/TP-2004-400*.

Verbelen F. (2019). "Meteor velocity derived from head echoes obtained by a single observer using forward scatter from a low powered beacon". *WGN, Journal of the IMO*, **47:2**, 49–54.

Handling Editor: Jean-Louis Rault
This paper has been typeset from a LaTeX file prepared by the author.

A Appendix STFT

The Short Time Fourier Transform has here the following form

$$\begin{aligned} \mathcal{A}_R(f_i - f, t) &= \int_{-\infty}^{\infty} A_R((2\pi f(t+t'), x(t+t'))e^{i2\pi(f_i-f)(t+t')}\text{HannWindow}(\alpha t')dt' \ , \\ \text{HannWindow}(w) &= \begin{cases} \frac{1}{2} + \frac{1}{2}\cos(2\pi w) & -\frac{1}{2} \le w \le \frac{1}{2} \\ 0 & |w| > \frac{1}{2} \end{cases} \ , \end{aligned}$$

where α determines the width of the window.

Meteor Beliefs

Was Mithras really 'born' from a meteorite?

Alastair McBeath [1]

In the February 2020 issue of this journal, a paper was presented proposing the ancient Roman god Mithras had been born not from an ordinary rock, but a meteorite (Sibley, 2020). That article however, featured selective evidence, often conflating outdated, sometimes inaccurate, ideas as support, some of which have been investigated previously in *WGN* and other IMO publications. No genuine evidence for such a meteoritic origin for Mithras can be traced from the information cited by Sibley. As many of the matters raised may be unfamiliar to *WGN* readers, a detailed examination of some of the more problematic elements is presented to help increase the understanding of such aspects within the meteor astronomy community, and perhaps assist in avoiding similar difficulties in future.

Received 2020 June 14

1 Introduction

Jane Sibley's article in *WGN* 48:1 (Sibley, 2020), suggesting scenes showing the later Roman Empire deity Mithras emerging from a rock could be reinterpreted as him emerging instead from a meteorite, while of minor interest, was flawed by some poor referencing and an over-reliance on unverified assumptions.

The Mithras mystery cult is certainly widely-attested from archaeological findings across the former Roman Empire's area in both military and civilian contexts, between the late 1st to late 4th centuries CE. However, much of its iconography, and almost all of its beliefs, are enigmatic, as there are few surviving written texts regarding it that provide significant detail, none of which were written by cult members. Consequently, since the first scholarly examinations of it in modern times, beginning in the late 19th century, the cult and its mysteries have become a source of unresolvable debate, onto which commentators have often projected whatever ideas of their own they wished to promote.

The standard introduction to studies of the subject now is "The Roman Cult of Mithras" (Clauss, 2000), a curious omission from Sibley's references, given some of the topics raised in the *WGN* article with insufficient explanation, such as Mithras' two common accompanist figurative humans, Cautes and Cautopates (*cf.* Clauss, pp. 95–98), or the unsourced use of the term "Leo grade", Leo or Lion being one of seven apparent 'levels' of cult membership, perhaps only for the cult's priests (see Clauss, Chapter 11). Another valuable, if purely online, introductory resource is the extensive series of webpages regarding Mithras and his cult, with many images of related objects, and a collection of English translations of ancient and medieval text-sections referring to Mithras, on the `Tertullian.org` website by Roger Pearse (Pearse, 2020; accessed March-June 2020).

Unfortunately, the UK's lockdown measures in response to the global COVID-19 pandemic from March 2020 created difficulties in checking those sources Sibley cited which I did not have copies of to-hand, and which were not readily accessible online. Of those, the only especially problematic text was the second volume of Vermaseren's *Corpus Inscriptionum et Monumentorum Religionis Mithriacae* (CIMRM), published in 1960. Luckily, the first volume (Vermaseren, 1956) is freely available online *via* the Archive.org website for those without physical access, while a useful number of objects from both volumes are shown with images – often of better quality than those available to Vermaseren – with CIMRM text-extracts, on the `Tertullian.org` website. As CIMRM Vol. 1 covers only up to Monument (Mon.) 1002, gaps in the current coverage at `Tertullian.org` meant it was not possible to check the details for CIMRM Mon. numbers 1036, 1113 and 1340 from Sibley's Note 3, 2198 from Note 11, and 1016, 1147, 1204 and 1268 from Note 16.

The remaining 35 CIMRM items referred to were checked, a level of detailed confirmation felt necessary due to the lack of images in the article, and the number of referencing errors uncovered from early in the process. The most obvious of those was on page 23 of the *WGN* paper, Figure 2 there, captioned as CIMRM Mon. 695, yet labelled on the image as actually being Mon. 860. Of the 47 citations to CIMRM items available for checking from the article's Notes (eleven featured two or three times), 28 were found to be inaccurate, about 60%, as not showing what they were claimed to. Four – Mon. 144, 428, 532 and the lion-headed figure from the fragmentary relief 1510 – were not imaged in CIMRM at all, allowing no confirmation of what they contained.

2 Images of Mithras' rock-birth

Disturbingly for a paper supposedly concerned primarily with Mithras' rock-birth, just ten of the supporting CIMRM items were mentioned as showing it in Sibley's Notes. Of the seven that could be checked, three were incorrectly cited, CIMRM Mon. 428 (from Note 3 – not imaged), 557 (Note 3 – this showed a stone carving of a clothed woman's upper torso with a (possibly wrongly) restored head, surrounded by textured

[1] 12a Prior's Walk, Morpeth, Northumberland, NE612RF, England, UK. Email: `mcbal.gwyvre@gmail.com`

IMO bibcode WGN-484-mcbeath-mithras
NASA-ADS bibcode 2020JIMO...48..118M

rock, and may have been part of a largely lost surround to a bull-wounding scene originally, as that act was sometimes shown as happening in a subterranean, rocky cave), and 695 (caption to Figure 2 and Note 18, as mentioned already; on CIMRM 695 see also the section on 'Phanes' below). However, in just the first CIMRM volume (Vermaseren, 1956), twenty items described as showing this rock-birth scene were quite easily identified, albeit three were not imaged there, of which Sibley had referenced only five (including the unimaged Mon. 428). A further 25 images of, or including, Mithras' rock-birth were found from the second, 1960 volume of CIMRM *via* the `Tertullian.org` website, of which one featured in Sibley's Note 16, Mon. 1247, where it was wrongly cited in support of smooth sandstone balls having been found loose in a number of *mithraea* (the subterranean temples dedicated to Mithras, sometimes set wholly within a cave). CIMRM Mon. 1247 is actually a double-sided red sandstone pivoting relief sculpture, showing numerous scenes from the Mithras mythological iconography, including the rock-birth.

Adding in another nine rock-birth scene images from the `Tertullian.org` website discovered since the second CIMRM volume was published, raised the total of readily-accessible Mithras rock-birth items to 54, 51 of which were imaged. Clearly, cherry-picking a handful or so from these could create a false impression of anything the remainder might demonstrate, while a thorough review of **all** available materials, both written and iconographic, would be essential when trying to prove any exceptional theory, such as the rock-as-meteorite scenario Sibley favoured.

If we take the rock-births as showing Mithras' earliest acts, thus picturing him at his youngest, even a cursory examination of the available rock-birth art shows him to be only rarely associated directly with anything loosely 'celestial' then. Indeed, despite the pluralisation, even Sibley recorded just one item, CIMRM Mon. 985, in support (Figure 1 here). Whether even that confirms the notion of Mithras being intended as shown in the celestial plane is a matter of personal interpretive belief. Others have seen this relief as Mithras supporting the heavens from beneath, turning the heavens, or using the heavenly arch to help him climb out of the rock at his birth. The presence of the earthly animals, and the probable cardinal winds, at least confirms this is not a purely celestial setting (*cf.* Clauss, 2000, pp. 68 & 70, including Figure 29 on p. 68).

Figure 1 – A Mithras rock-birth carved relief, 0.73 m tall, 0.25 m wide, 0.12 m deep, found at Trier, Germany in 1928. The god, wearing only a Phrygian cap, is posed as if climbing above, or out from, a rocky mountaintop while three of his frequent animal accompanists, a bird (often suggested as a raven), a snake and a dog look up at him from the rocky landscape. He holds a large globe in his left hand, while his raised right rests on the edge of a circular ring with six zodiacal figures on it (clockwise, these appear to represent the constellations of Aries, Taurus, Gemini, Cancer, Leo and Virgo). Four heads, probably of the four figurative cardinal winds, are set around this ring, the whole group placed between two temple columns, with a triangular pediment above. The pediment contains carvings of a seated lion, a slightly damaged double-handled cup, possibly with a snake wound around it (Vermaseren's suggestion), a spindle-shaped object (possibly representing a thunderbolt, again according to Vermaseren) which rests at an angle against a globe with two crossed bands around it, with an indeterminate oval or wedge-shaped object with a central 'U'-shape carved into it partly in front of the globe (perhaps an unlit torch). Above the narrow ends of the pediment are two more heads, that to the top left the figurative radiant Sun, that to the top right badly damaged, but likely intended as the Moon, from similar Mithras-associated groups. Described as Mon. 985 in Vermaseren (1956, pp. 327–328 and Figure 237). This image by Carole Raddato from Wikimedia Commons.

3 The celestial Mithras elements

Astral components are relatively common in the Mithras iconography overall, especially scenes showing him wounding or killing a bull. These may include a partial or complete set of zodiacal figures as known to the ancient Romans, and images of the figurative Sun and Moon, as already suggested by Figure 1. Sometimes there may be stars, and rarely a crescent, on Mithras' cloak, with occasionally more stars in the field behind him in the bull-wounding scenes (and despite these often being set within a cave; the cave itself may be representative of the cosmos Mithras had created, however – see below). Such features may have had an astronomical or, more likely for the period, an astrological significance for cult members, although they may have been meant as symbols indicating cyclical time too. Roger

Beck (2006) for example, proposed a detailed explanation for these and other features, including the internal layout of the mithraea, which may have involved especially the region of sky around the six zodiacal constellations named in the Figure 1 caption, and some of their neighbours, such as Canis Major and Minor, and Hydra, along with the importance of cyclical time again.

Beck also provided several quotes from the 3rd century CE Neo-Platonist writer Porphyry's work *De antro nympharum* ('The cave of nymphs') 6, from the 1969 restored translation. The following citation is from Beck (2006), p. 102, omitting here the inserted original Greek text highlighting. Porphyry was writing about the nature of the mithraeum:

"Similarly, the Persians call the place a cave where they introduce an initiate to the mysteries, revealing to him the path by which souls descend and go back again. For Eubulus tells us that Zoroaster was the first to dedicate a natural cave in honour of Mithras, the creator and father of all; it was located in the mountains near Persia and had flowers and springs. This cave bore for him the image of the Cosmos which Mithras had created, and the things which the cave contained, by their proportionate arrangement, provided him with symbols of the elements and climates of the Cosmos. After Zoroaster others adopted the custom of performing their rites of initiation in caves and grottoes which were either natural or artificial."

Beck's discussions included the ahistorical use of Zoroaster, and the likely mythical origin of the first cave sanctuary. However, the central importance of subterranean and cave sanctuaries to the Mithras cult is undoubted, while the comment regarding cult initiates learning of souls descending and returning while in a 'cave' themselves could easily account for the Mithras rock-birth sculptures and scenes without involving more speculative reasoning.

Porphyry had a little more to say about Mithras' astral associations and the mithraeum in *De antro nympharum* 24, here again from Beck (2006), p. 107, this time without the separation of the lines and their numeration used there for the purposes of Beck's book:

"To Mithras, as his proper seat, they assigned the equinoxes. Thus he carries the knife of Aries, the sign of Mars, and is borne on the bull of Venus; Libra is also the sign of Venus, like Taurus. As creator and master of genesis, Mithras is set on the equator with the northern signs on his right and the southern signs to his left. They set Cautes to the south because of its heat and Cautopates to the north because of the coldness of its wind."

Beck's thesis may not be correct, and earlier translations of Porphyry may use variant wording in places, or other differences (the final sentence regarding Cautes and Cautopates in the *De antro* 24 quote is a restoration, for example). Regardless, to attempt a discussion of Mithras' astral aspects and not even mention such textual information as Porphyry exists, again seems too much like cherry-picking facts to fit a theory.

David Ulansey's 1989 text that Sibley did refer to in-passing, while the only other detailed work that tries to explore the astronomical and astrological elements of the Mithras cult, is not well-regarded among Mithras scholars. Partly this seems to stem from their own uncertainties about such matters, though a large part descends from the, at times imaginatively speculative, nature of Ulansey's thesis, much of which has no evidential basis. His early chapters exploring the history of modern studies of Mithras are in general sound and useful though, and his theory's starting point (Chapter 3), that rather than being merely Persian, Mithras was actually **Perseus**, is an intriguing idea, particularly given the apparent significance of the Aries-Taurus to Virgo stretch of sky in the cult's imagery.

Indeed the idea of Mithras originating from ancient Persian beliefs seems doubtful, given that what we know of the Persian deity Mitra or Mithra seems wholly unrelated to the imagery of the Roman Mithras cult, beyond both being solar gods (*cf.* Clauss, 2000, Chapter 1). The Assyrian-Persian-modern Zoroastrian winged disc, noted by Sibley (2020) p. 21, for instance, features nowhere in known Mithras-associated art. The ancient Romans may have simply invoked 'Persia' as a semi-mythical, very ancient, and thus mystical, setting to lend credence to the importance of their cult, much as they had done previously with Phrygia in west-central Anatolia regarding the Magna Mater stone, for example (see McBeath & Gheorghe, 2005, p. 139).

4 Meteorites & other sky-fallen objects

Contrary to Sibley's repeated assertions that the ancient Romans apparently enjoyed an understanding of meteorites equal to that held by scholars only after the early years of the 19th century more modernly (essentially beginning *circa* 1803 CE; *cf.* Beech, 1994, 1995 and Knöfel & Rendtel, 1994 in this journal alone), it is actually clear that the ancient Greeks, Romans and associated cultures of the Classical to early Medieval periods believed a great many different kinds of object could fall from the sky, such as earthly stones, fire, wood, fossils and human-crafted objects made of stone (*cf.* McBeath & Gheorghe, 2004, 2005 & 2009). Consequently, suggesting they could have recognised genuinely meteoritic features such as regmaglypts, and understood them to be anything more than typical shapes on the surface of ordinary earthly stones, makes no sense, while proposing such forms were thought the finger-marks of a deity is without foundation.

Of the four supposed meteorites cited in support of this 'finger-marks' notion, one, from the Temple of Diana at Ephesus, has been dealt with in these pages previously (McBeath & Gheorghe, 2005, pp. 141–142). The only evidence the image of the goddess Diana at this temple was believed sky-fallen comes from the biblical *Acts of the Apostles* 19:35–36, and even that does not mention a stone object in the original Greek, let alone describe it.

Astarte of Tyre's prominence, such as it is, devolves to a short passage in the 3rd/4th century CE Christian writer Eusebius of Caesaria's work *Preparation for the Gospel*, Book I, Chapter I.38c:

"Astarte set the head of a bull upon her own head as a mark of royalty; and in travelling round the world she found a star that had fallen from the sky, which she took up and consecrated in the holy island Tyre." (Gifford, 1903, p. 43.)

Again, no meteoritic stone object, just something undescribed that had fallen from the sky without any intervention by a deity.

The two remaining objects, Amun from Thebes and Seth from Casaba, seem to derive solely from a series of papers regarding ancient iron published by G A Wainwright in various journals during the late 1920s and 1930s (*cf.* Wainwright, 1936). However, these were based on the unfounded assumptions that all ancient references to 'baetyls', 'thunderbolts' or sometimes just isolated sacred stones in or near temples, meant only 'meteorites', and that all pre-Iron Age iron objects or references to iron must have been purely meteoritic, something neither ancient written sources nor more modern archaeological findings support. To be fair, the meteoritic iron concept held sway, despite being unsupported by any reliable evidence, from the early 19th century through into the 1970s (*cf.* Larsen *et al.*, 2012, especially pp. 142–143). The Amun and Seth objects seemed to have been merely unidentified stones in temples.

5 Standing-stone worship and houses of gods

Stones were sometimes stated in ancient texts to have been the house of this or that deity. None that have survived to allow modern examination have proven meteoritic. From perhaps the 3rd millennium BCE, and certainly the 2nd onwards, some standing stones were worshipped across much of the ancient Near East, particularly around the Palestine region and neighbouring areas (*cf.* Scheyhing 2018). Again though, all the extant examples are of normal earthly rock types.

Unsurprisingly then, Sibley's four Jewish Masoretic Text/Christian Old Testament (MT/OT) references (from Note 5) failed to support a meteoritic origin or nature for such stones either. Genesis 28:11–19 recounts the tale of Jacob's dream of a stairway to heaven at a place called Luz. He slept there using a local earthly stone as his pillow. Waking in astonishment from his marvellous dream, he set up the pillow-stone as a pillar to mark the spot, and anointed it with oil (an act of worship), saying the place – not the stone – must be the house of God. He renamed the settlement of Luz as Bethel – literally 'house/temple of God' from the Hebrew – because of this. Subsequently (Gen. 28:22) he made a pact that if the god Yahweh looked after him as promised, the stone pillar should become that god's abode. The latter never occurred. When Jacob returned to Luz/Bethel in Genesis 35:1–15, the pillar was no longer mentioned, and he built a new altar to the god Yahweh there instead, calling the place – not the altar – El-bethel, 'God of the house of god' (Gen. 35:6–8).

Joshua 24:26–27 describes the setting-up of a large native stone found at Shechem under an oak or terebinth tree beside the sanctuary of Yahweh there, saying that as the stone has heard the words spoken to the Israelites by Yahweh, it shall be a witness against them should they deal falsely with their god. So this ordinary earthly stone has been granted numinous powers of hearing and speech as it chanced to be near where an important deity-related event had happened.

Leviticus 26:1 is one of numerous MT/OT passages prohibiting the setting-up for worship of idols, images, pillars and figured stones. Numbers 33:52 describes the driving-out by the Israelites of the inhabitants of Canaan, and the destruction of their figured stones, metal images and high places of worship. In combination with similar biblical sections, it becomes clear the worship of such objects – and wooden poles or sometimes living trees, called *asherah*, dedicated to female deities – was widespread both among the natives of Palestine/Canaan and the incoming Israelites. Not once is there any suggestion these objects were recognised as even fallen from the sky, let alone being genuine meteorites.

6 Diopet & meteoritic iron

Kenneth Oakley's paper *The Diopet of Ephesus* (Oakley, 1971) was an odd source for Sibley (Note 5) to cite in support of fallen meteorite worship. From p. 207 there: "It is widely believed by classical scholars that baetyli were sometimes meteorites, but so far as I am aware in *no* instance has this ever been proved" [original emphasis]. After discussing the human-carved earthly greenstone Neolithic pounder suggested as being the diopet (an ancient Greek term used with objects believed fallen from the sky; see McBeath & Gheorghe, 2005, especially p. 135), Oakley commented on the numbers of such prehistoric hand-crafted stone implements across Europe that were known as 'thunderstones', as believed to have come from the sky. He added that, "on rare occasions the ancients must have encountered actual meteorites and regarded them too as 'thunderstones' " (p. 211), due to the earliest iron artifacts being of meteoritic nickel-iron. While not all early iron objects have proven to be meteoritic, this statement is overall reasonable, especially for iron meteorites, as their numbers recovered modernly are depleted from the more heavily-populated, agriculturally-active, parts of the Old World, as compared with places like the Americas, Australia and South Africa, from pre-modern times. This suggests such readily-recognised metallic lumps found lying on or near the surface could have been taken as 'gifts from the gods' by previous generations without ever being seen to fall, and gratefully employed for tool-making and the like subsequently (*cf.* Larsen *et al.*, 2012, especially pp. 142–143, while on the difficulties in analysing ancient iron objects to identify their true origins, see Johnson *et al.*, 2013). As for Oakley's 'diopet', it may not have been excavated at Ephesus at all, as the circumstances of its discovery were not recorded by it modern finder (Oakley, 1971,

p. 210, note 3). Thus its identification is at best suspect concerning any link with the Temple of Diana at Ephesus. In regard to the 'baetyli', see further below and the notes under 'Betyls and other sacred stones' in Hendrix *et al.*, 2012, pp. 81–82.

7 Zeus Kappotas

Leaving aside other secondary sources in Sibley's Note 5 as adding little to the discussion, perhaps including the unlisted reference "Sears (1978)", the specific reference to "Zeus as a meteorite" attributed to page 13 of Blinkenberg's *The Thunderweapon in Religion and Folklore* (1911), devolves to the 2nd century CE Greek author Pausanias' comments on a native, unworked stone about three stades ($\sim$ 555 m) from Gythium in Laconia (*Description of Greece* Book III.22.1) which he said was called Zeus Kappotas. 'Kappotas' remains a unique term of unknown derivation, plausibly a local Doric word or pronunciation. Pausanias took it to mean 'Reliever', as Orestes was thought to have been relieved of his madness by sitting on the stone, not the only place to claim this distinction according to Pausanius' writings. The stone has never been located since.

Blinkenberg repeated a suggestion from elsewhere that the whole name may have meant "Zeus fallen (from the heavens)", which he noted as meaning lightning, though he then suggested this would have "more probably been a meteor" [*sic*]. However, his supporting evidence for this meteorite hypothesis (a 1741 Dutch reference in his Sources 107 & 108; Blinkenberg, 1911, pp. 102–103) came down to just two supposed events, the fall of a 3.5-feet long 'meteorolite' in Devonshire, England in 1622, regarded as a thunderstone, and another 'thunderstone', 1.5-feet thick, at a church in Grave, The Netherlands, which he only suggested **might** have been also a 'meteorolite'. Despite the year being apparently one out, as England did not adopt the Gregorian calendar until 1752, the Devonshire event was probably the plausible meteorite fall at Stretchleigh, Devon on 1623 January 10 Gregorian. It happened in daytime near a group of men working in an orchard. The object was described as $\sim$ 3.5 feet long, 2.5 feet broad and 1.5 feet thick ($\sim 1 \times 0.75 \times 0.45$ m). The Stretchleigh stone was broken-up for souvenirs and lost soon after its arrival, so its true nature remains unconfirmed. The surviving local notes about it said it arrived with a fearful, loud noise, likened to cannon-fire, not thunder (Robinson, 2010, pp. 99–100). In any case, these two possible meteorites can be scarcely used as support for the beliefs current in ancient Greece $\sim$ 1500+ years earlier, especially as Blinkenberg went on to detail (1911, p. 14) how the ancient Greeks had consecrated sites struck by lightning to this "descending Zeus", 'Zeus Kataibates', referencing supporting Greek texts in his Source 115e on pp. 110–111. On page 111 he further related the ancient Greeks thought lightning could bring madness, hence the lightning god Zeus could also cure it. A more recent discussion of the Gythium stone is in Gaifman (2010, pp. 79–80), who suggested the name was from a purely local cult, again possibly one where Zeus was thought to have 'sent down' a cure for Orestes' madness, if 'Kappotas' was indeed the local variant of *kata-potas*, 'fallen down', 'descended', which is still unproven.

8 Jupiter Lapis & the Magna Mater stone

Next, Sibley reinterpreted 'Jupiter Lapis' as meaning 'Jupiter-as-a-stone', apparently to indicate it was both the house of the god and a meteorite. However, ancient sources demonstrate there was not just one stone involved, and that in the recorded cases, the stone was a small, ordinary one, picked up, used and discarded solely for the occasion, as rather than referring to a specific object, it was actually a process, *per Jovem lapidem jurare*, 'to swear by Jupiter Lapis', which was used when a particularly important oath was to be made. The most detailed description was given by Polybius in his *Histories* III.25, discussing treaties made between Rome and Carthage in 279 BCE, when the Romans needed to swear by Jupiter Lapis to show the seriousness of their promise:

"The oath by Jupiter Lapis is as follows. The man who is swearing to the treaty takes in his hand a stone, and when he has sworn in the name of the state, he says, "If I abide by this my oath may all good be mine, but if I do otherwise in thought or act, let all other men dwell safe in their own countries under their own laws and in possession of their own substance, temples, and tombs, and may I alone be cast forth, even as this stone," and so saying he throws the stone from his hand." (Paton, 1922, p. 61.)

The small, black, potentially meteoritic stone which formed the face of an otherwise undescribed image of the Magna Mater, Sibley's "head of a silver statue of the goddess Ops (Cybele)", was already discussed in detail by McBeath & Gheorghe (2005, pp. 137–140).

9 Baetyl, Bethel & thunderstones again

Returning now to the ancient Greek term 'baetyl', this has been often conflated with the Semitic name Bethel since late Antiquity and early Medieval times. The matter remains unresolved and problematic, not least because both words appear to have had several different meanings anciently. Many modern commentators have continued and contributed to the confusion, such that 'betyl' or its homonymic can be used now as a general term for any seemingly once-important and perhaps revered, usually aniconic, stone object. Sometimes, albeit less so now than formerly in near-modern times (that is, after the early 19th century CE), such 'betyls' were commonly assumed to have been meteorites, and probably ones that had been seen to fall, despite the complete lack of supporting evidence for either point.

Ironically, the earliest use of the Greek term may be that in Pliny's *Natural History* 37.51, a Latin author who in this instance had preserved a précis of what he attributed to an earlier Greek writer Sotacus, whose work on the matter is otherwise lost. Pliny lived from

23–79 CE, and while we have no firm evidence for Sotacus' lifetime, it has been suggested he may have written his text sometime around or after the early 3rd century BCE (e.g. Faraone, 2014, p. 1).

Pliny's notes discussed a number of rock-crystal-like stones that he said shone from within like a star, sometimes the Moon, or once even the Sun, when catching the light, in the text leading into the 'betyl' section (*Nat. Hist.* 37.48–51; see Eichholz, 1962, pp. 272–275, whose notes on pp. 272–273 suggested some may have been varieties of moonstone, and perhaps cat's-eye quartz). Two of those stones, one an inferior type, the other having a brilliant blue sheen, he called *ceraunia*, meaning 'thunderstone', from the Greek *keraunion*, 'thunderbolt'. After discussing a third kind of ceraunia, dull, but revealing a twinkling star within when soaked in vinegar for a time, attributed to another earlier author Zenothemis, Pliny continued:

"Sotacus distinguishes also two other varieties of the stone [= ceraunia], a black and a red, resembling axe-heads. According to him, those among them that are black and round [or rounded] are supernatural [or sacred] objects; and he states that thanks to them cities and fleets are attacked and overcome, their name being 'baetuli', while the elongated stones are 'cerauniae'. These writers distinguish yet another kind of 'ceraunia' which is quite rare. According to them, the Magi hunt for it zealously because it is found only in a place that has been struck by a thunderbolt [or by lightning]." (Eichholz, 1962, pp. 274–275, with clarifications/amendments by the current author in '[ ]' brackets.)

This seems to suggest a variety of different kinds of stone or stone object were believed associated with thunderstorms, including those called baetuli that looked like rounded black axe-heads. It seems plausible this is the first written record of what was, or at least became, the pan-European practice of using polished Neolithic stone axes, known as 'thunderstones', as amulets to protect life and property against lightning strikes. Such a practice, supported by archaeological and textual evidence (from the Roman period and the 5th century CE respectively), has persisted in parts of Europe into contemporary modernity (*cf.* Faraone, 2014, especially pp. 1–3). Certainly by Roman times, there are such axes inscribed with magical texts and symbols, along with figurative illustrations of deities, as Faraone's 2014 paper discussed in detail, including an example showing the Mithras bull-wounding scene (Figure 2, p. 5 there).

The next appearance of the Greek term, as *baitylos*, occurs in a fragment of a text attributed to Philo of Byblos (lived *circa* 15–10 BCE to 45–50 CE). This survives only in a later work, *The Preparation for the Gospel* by Eusebius of Caesaria, which we met briefly earlier when commenting on Astarte of Tyre. Eusebius' complete lifetime is uncertain. He is though known to have died *circa* 339 CE. The relevant section is from Book I, Chapter X.37d: "the god Uranus devised the Baetylia, having contrived to put life into stones." The Greek text confirms the distinction between the usual *lithos* for 'stone' and *baitylia* for the magical, living stones (English translation from Gifford, 1903, p. 42; Greek text for the passage from the edition by Dindorf, 1867).

After this, the only other detailed notes on the baitylos, now joined by the diminutive form 'baitylion', often translated as 'baetylets', 'little baetyls', are found in a Greek work by Damascius (*circa* 467–540 CE), known in translation as either 'The Philosophical History' or 'The Life of Isidore', as much of the surviving text is concerned with the studies, travel and work of Damascius and his contemporary colleague Isidore. For more details, see the text and translation used here by Polymnia Athanassiadi (1999).

There are two sections in this work that involve baetyls, one of which, 72F (Athanassiadi, 1999, pp. 188–189) is preserved only as a summary comment by subsequent writers. The gist of this segment is that one of Damascius' and Isidore's teachers, Asclepiades, had ascended Mount Lebanon in Syria, near Heliopolis there (modernly Ba'albek, Lebanon; Talbert, 2000, p. 1062), where he saw many baetylets or baetyls, and returned to relate many 'monstrous tales' about them that Damascius' redactors were unwilling to retain and share.

The later passage, 138 (Athanassiadi, 1999, pp. 308–311), survives almost complete, and records an occasion when Damascius and Isidore together encountered a baetyl on or near Mount Lebanon themselves. Damascius writes: "I saw the baetyl moving in the air, now hiding itself in the clothes of its guardian, now held in his hands." This 'guardian' was a man named Eusebius (not the Eusebius we have already met, however). This Eusebius related that he had wandered off from Emesa (modern Homs, Syria; Talbert, 2000, p. 1045) one night to the mountain on an impulse. Sitting to rest at its foot, "He then suddenly saw a ball of fire leaping down from above and a huge lion standing beside it, which instantly vanished. He ran up to the ball as the fire was dying down and understood that this was indeed the baetyl; picking it up, he asked it which god possessed it, and the baetyl answered that it belonged to Gennaios (the Heliopolitans honour Gennaios in the temple of Zeus in the shape of a lion). He took it home that same night, covering, as he said, no less than two hundred and ten stades [$\sim$ 40 km]. Eusebius was not the master of the baetyl's movement, as is the case with others, but he begged and prayed and the baetyl listened to his incantations."

The baetyl was then described. "The stone was a perfect sphere, whitish in colour and a span in diameter [$\sim$ 22 cm]; its size was sometimes larger, sometimes smaller, and on occasions it acquired a purple hue." Eusebius indicated there were inscribed letters on it, coloured with vermillion, which it used to pass oracles to an enquirer. He could strike it against a wall, so the stone would emit a soft whistling sound that he could interpret. Damascius noted he felt the stone to be divine, Isidore that it was demonic, though only of a minor, fairly harmless, type. Damascius' last comment was that each baetyl was ascribed to a specific god, including Cronus, Zeus and Helios, among unnamed others.

Some might find much of this fanciful and ridiculous. Damascius' redactors clearly thought so, judging by their pithy interjections at times, omitted from the above notes and citations. It is though obvious that a world where such things were felt possible was that which Damascius, Isidore, their colleagues and mentors inhabited, as noted in many other parts of Damascius' text. For example, another of Damascius' teachers, Heraiscus from Egypt, was credited with an extraordinarily intuitive perception, such that he could distinguish between ordinary, inanimate sacred statues and those – otherwise identical to an onlooker – which were infused by divine inspiration from a particular deity (*Phil. Hist.* 76D-E; Athanassiadi, 1999, pp. 194–197). Which of course also tells us that period beliefs indicated a statue might be just stone, or be possessed by a deity, though in neither case was it called, or anything like in appearance, a baetyl.

Nor were any of these baetyls said to have fallen from heaven, whether as the act of a deity or not. Pliny's ceraunia were linked to thunderstorms and lightning strikes certainly, albeit so were other things anciently, such as mushrooms (Plutarch, *Quaestiones Conviviales* Book 4, Question 2; *cf.* the discussion in Beech, 1993). None of the objects described seem likely candidates for potential meteorites either, and none were said to have been worshipped. We might perhaps reinterpret Eusebius' 'ball of fire leaping down from above' in Damascius' text as meteoric, or possibly meteoritic, if in a very garbled form. However, as that Eusebius was at the base of Mount Lebanon at the time (probably somewhere in the northern mountains of modern Lebanon), the phrasing was more likely a reference to the fire descending from higher up the mountain, potentially – if real – a form of ball-lightning, such as that associated with rock-stress piezoelectrical activity, sometimes called 'earthquake lights'. It was not the only recorded event of unusual moving lights on this named mountain anciently; see Athanassiadi, 1999, note 365 on p. 309, and references.

As mentioned though, the topic of the baetyl-stones does not exist in isolation.

A Semitic deity whose name transcribes as Bayt-el or Bayt-il, is known from two cuneiform treaties of the Assyrian King Esarhaddon, the first of which can be dated reasonably precisely to 675/674 BCE (*cf.* Pritchard, 1969, pp. 533–534, 'Treaty of Esarhaddon with Baal of Tyre'). Bayt-el appears in both with his consort Anat-Bayt-el. One or both names then recur occasionally as theophoric elements in recorded personal names from Mesopotamia in the 6th century BCE, and among the Jewish community at Elephantine in Egypt during the 5th century BCE. The biblical text of Jeremiah 48:13, "Then Moab shall be ashamed of Chemosh, as the house of Israel was ashamed of Bethel, their confidence" (Grudem, 2008, p. 1457), suggests a deity named Bet-'el, as transcribed from the Hebrew MT, may have been worshipped at an earlier time by the Israelites too, given that Chemosh was the leading god of Moab.

Shortly before mentioning the living-stone baitylia, Philo's text according to Eusebius contained this information regarding the gods (Gifford, 1903, p. 41, from Eusebius I.X.36b-c): "Uranus, having succeeded to his father's rule, takes to himself in marriage his sister Gé, and gets by her four sons, Elus who is also Kronos, and Baetylus, and Dagon who is Siton, and Atlas." Despite their relative textual proximity, no connection was made by Philo/Eusebius between the deity Baitylos and the living-stone baitylia at all, although this has not prevented subsequent commentators from supposing such a link. The matter remains unresolved.

Three 3rd century CE Greek inscriptions from Syria are to a deity or deities whose name includes the transcribed element 'betylos' or 'baitylos', of which the more relatively helpful with other information is an altar from Dura Europos (now Salihiya on the Euphrates in eastern Syria – Talbert, 2000, p. 1303; imaged with details and a translation of the inscription online in April-May 2020 at `http://arachne.uni-koeln.de/item/objekt/220868`). The translated text includes the dedication: "To (his) national god Zeus Betylos, (god) of the dwellers along the Orontes". The River Orontes, now the Nahr el-Asi (Talbert, 2000, p. 1033), runs through western Syria.

Aside from these Near Eastern deities, and the various Greek, sometimes living, stones, Bethel/Bet-'el was also used biblically as a place-name, meaning 'house of god' from Genesis 28:11–19 as remarked earlier. Its use there suggests what became the abode was originally an otherwise unremarkable open place, given significance only after the extraordinary event of Jacob's dream-vision had happened there. It was so ordinary a spot, it needed to be marked to indicate its importance by erecting a local stone as a pillar, in the Hebrew MT a *masseba*, or merely a *lithon* from the Greek Septuagint version. The renaming of the nearby settlement of Luz as Bethel by Jacob became a logical corollary, to the point where, as Genesis 28:22 has it, the ordinary stone pillar could be imbued with the numinous power of what has become the sacred place, so it too might be renamed as the house of god. Genesis 35 notwithstanding, it seems likely that this is the reason the conflation by late Greek and Latin lexicographers and mythographers between some of the Greek baitylos stones – those connected with particular deities, say – and the Semitic cult of stone-worship occurred. This may have been because at some prior point the Greek-speakers had adopted the word from the Semitic, perhaps due to its meaning 'house of god'. There seems not to be any earlier precedent term in Greek, at least. We may never know definitively.

For unreferenced notes on the baetyl/Bethel discussion in this section, see also Scheyhing (2018) and the essays by S. Ribichini ('BAETYL', pp. 157–159), W. Röllig ('BETHEL', pp. 173–175) and M. C. A. Korpel ('STONE', pp. 818–820) in van der Toorn *et al.* (1999). Despite its date, it is also worth reviewing George Moore's 1903 paper "Baetylia" on the stone types, and the importance of not confusing these with

the worship of stones, a sensible commentary which has been too-often ignored since.

It was surprising in light of the preceding discussions to find Sibley (2020, p. 21) claiming that a "triangular/coniform meteorite was revered as a *baetylos* in the fifth century BCE Greek city of Caria, Kaunos; a stone answering this description was recently excavated at that site". Disappointingly, the only possible source for this remarkable, hitherto unknown, discovery from the relevant Note 7 was the unlisted "Konuk (1988), pp. 222–223". This though was most probably Koray Konuk's paper *The Early Coinage of Kaunos*, published in 1998 (Konuk, 1998), as on page 223 of that we learn of the discovery in the remains of a fourth century BCE temple at Kaunos (now Dalyan, Turkey; Talbert, 2000, p. 998, 'Caunus') in 1991 "of a large conical piece of limestone broken into two parts." Its size when whole would have been more than 4 m tall and 1.5 m wide, with its lower part standing on the bedrock and buried so that only the upper $\sim$ 2.5 m would have been visible. It was suggested, partly on the coin evidence showing a triangular object thought to have been this stone, that it had been erected in the 5th century BCE, with the temple later built around it. The earliest coins found showing such an object can be approximately dated to within a couple of decades of *circa* 490–470 BCE. Konuk did fall into the trap of later calling the stone a baetyl, albeit purely in the modern sense of it having been a worshipped stone. Its location in coastal southwestern Anatolia makes it simply a western example from the zone where setting-up and revering such standing stones had existed across the Near East since the 2nd millennium BCE, or perhaps before, maybe $\sim$ 1500+ years before the Greeks had used 'baetyli' for some kinds of stone object. So the count of worshipped meteorites known to have existed among these ancient standing stones remains firmly stuck at zero.

10 Lion-headed figure

It is uncertain what Sibley's comments on matters such as the lion-headed human, the deity Phanes, pine cones and small carved stone balls or representations of globes were intended to add to the Mithras-emerging-from-a-meteorite idea.

Certainly, some scholars have opted to call the lion-headed figure found in a number of mithraea 'Aion', albeit based on very flimsy evidence, given that the only sculpture probably of it with a name carved on reads "Arimaniu. . . ", even if that may be the partial name of the statue's provider, not the creature. The sculpture is detailed as CIMRM Mon. 833–834 by Vermaseren (1956, p. 290, but not imaged there; see instead 'The Lion-headed god' page on the `Tertullian.org` website (Pearse, 2020), as that does have an image). The three fragmentary artworks known where Aion is identified by a Greek caption are all of a human-headed figure (see Pearse, 2020, *loc. cit.* for images). Such a fully human figure may be shown in artworks holding a large ring taller than himself with zodiacal figures along it, possibly indicative of cyclical time, since as his name suggests, he represents Eternity or Ageless Time. He is sometimes considered the same as the ancient Greek god of Time, Kronos, notably in the Orphic teachings. Aion has no known textual connection with Mithras, however, while aspects of the lion-headed creature can be associated with a variety of other ancient time-related deities as well – *cf.* Clauss (2000), pp. 162–167.

11 Phanes

A figure who may be Phanes is associated with a zodiacally-figured ring too in a 2nd century CE sculpted relief, a ring which surrounds him (CIMRM Mon. 695, pp. 253–254 and Figure 197 in Vermaseren (1956); see also the 'Mithras and Phanes' and 'CIMRM 695' pages of the `Tertullian.org` website (Pearse, 2020) for more details and better images). There, the central, naked, human male figure, possibly of Phanes, has cloven hooves for feet, a pair of wings, a small lion's face in the middle of his chest, and is wrapped around by the coils of a large snake. Above his head is what seems to be half an eggshell with flames coming from inside it, while five rays extend horizontally to either side of his head, three to his right, two to his left. A similarly-shaped half-egg-like object is set below his feet, again with flames coming from within it. In the Orphic cosmogony, Phanes hatched from the bright white world-egg that Kronos had created. In doing so, Phanes became the creator of all life, the gods and the universe as we know it – his name means 'make appear'. A pair of inscriptions found at Rome are dedicated to Helios-Mithras-Phanes (one begins with 'Zeus-' before Helios), and there are comparable lists of elements in period texts by Zenobius (*Proverbs*) and Theon of Smyrna where Theon has substituted 'Phanes' for Zenobius' 'Mithras'. The unique Mithras-emerging-from-an-egg sculpture from Housesteads in England, Sibley's Figure 2, has been suggested as originally a Phanes sculpture reused by the Mithras followers there. Regardless of the sculptures, it seems at least Phanes does have some definite, if loose, written links to Mithras. See also Clauss (2000), pp. 70–71 & 165–167.

12 Pine cones

Sibley's preference for calling what are often quite clear representations of stone pine (*Pinus pinea*) cones in ancient Roman art 'pineapples', seems strange, as that fruit was unknown beyond southern and central America before the 15th century CE. Such pine cones, both artwork and real, have been found in a great many places across the former Roman Empire, including in mithraea and funerary settings, along with numerous other military and civilian settlement contexts. The actual cones may be intact and whole, burnt (used perhaps as an air freshener and incense), or partial, with sometimes just the nuts recovered. The pine nuts were used as food at the time. Examples from Britain are particularly noteworthy, since as the stone pine was not native to the British Isles, all the actual cone remains recovered archaeologically from such sites must have been

imported. See for instance LiDonnici (2001) and Lodwick (2015), and in relation to Mithras, Clauss (2000), pp. 97–98 & 126. Nothing from any of these finds supports the possibility such pine cones were meant to somehow represent or substitute for genuine meteorites.

13 Stone balls

Plain globes of various sizes are seen in association with Mithras or his accompanists in a number of artworks, along with loose, small stone balls located with insufficient context from a few excavated mithraea. Mithras himself may hold a globe at his rock-birth, as Figure 1 here shows, which at the very least discounts Sibley's idea of this being some kind of representation of a meteorite in which Mithras had travelled to that birth. Where coloured artwork examples have survived, the paint on the globe is usually mid-blue, and while this may have been meant as a representation of the sky, it is perhaps as likely it represented instead the Earth as understood by the seafaring ancient Romans. The belt or crossed belts seen fitted around some of the globes (like that in the pediment of Figure 1), remain curiosities. The celestial ecliptic or equator have proven popular explanations for these among scholars, while the textual connection between Mithras and the equinoxes noted earlier perhaps provides support that the twin crossing points of ecliptic and equator each year is what the image of the two crossed belts was indeed intended to indicate. The lack of context for the excavated loose balls makes identifying their purpose currently impossible.

The comments in Sibley's Note 14 seem to imply these spheres, possibly only when held by a deity, were somehow to be considered as meteorites, although just a solitary example was claimed there, as "Zeus holding a meteorite", sourced to Plate 35 in Arthur Cook's monumental work *Zeus: A Study in Ancient Religion* (Cook, 1925, Plate XXXV facing p. 759). That Plate shows two views of a small marble statue, around 0.6 m high, a seated figure of Zeus on a throne. His left arm is upraised, while his right lies along the arm of the throne, palm open and up, with a small sphere resting in the palm. However, as Cook's note 2 on page 759 described, the lower right arm below the elbow had been completely restored modernly, and in his text on page 760, he noted the globe was added purely by the restorer, suggesting it should originally perhaps have been a figure of Victory instead. In light of Sibley's desire to 'see' meteorites when the word 'thunderbolt' was used, Cook's comment about this statue, that "the thunderbolt is nowhere to be seen" (*ibid.*) seems instructive.

14 Conclusion

Bearing in mind the preference for subterranean locations, including caves, for the mithraea celebrating the cult of Mithras in the Roman Empire, the artwork representations of caves enclosing Mithras' bull-wounding activities, together with textual information suggesting that the teaching of cult beliefs may have led to the perception of entering a cave as symbolic of death, emerging from one as rebirth, it seems unlikely we need to look for anything so exotic as a meteorite-emergence to account for the scenes where Mithras is shown apparently coming out from a rock or rocks. A closer examination of the available materials and information, including past items published in this journal, might have prevented such a questionable concept from featuring here in the form it did at all.

References

Athanassiadi P. (1999). *Damascius: The Philosophical History, text with translation and notes.* Apamea Cultural Association.

Beck R. (2006). *The Religion of the Mithras Cult in the Roman Empire: Mysteries of the Unconquered Sun.* Oxford University Press.

Beech M. (1993). "The Makings of Meteor Astronomy: Part IV". *WGN, Journal of the IMO*, **21:4**, 200–202.

Beech M. (1994). "The Makings of Meteor Astronomy: Part VIII". *WGN, Journal of the IMO*, **22:6**, 214–217.

Beech M. (1995). "The Makings of Meteor Astronomy: Part IX". *WGN, Journal of the IMO*, **23:2**, 48–50.

Blinkenberg C. (1911). *The Thunderweapon in Religion and Folklore: A Study in Comparative Archaeology.* Cambridge University Press.

Clauss M. (2000). *The Roman Cult of Mithras: The God and his Mysteries (Translated by R. Gordon).* Edinburgh University Press.

Cook A. B. (1925). *Zeus: A Study in Ancient Religion. Vol. II Zeus God of the Dark Sky, (Thunder and Lightning). Part I Text and Notes.* Cambridge University Press.

Dindorfius G. (1867). *Eusebii Caesariensis: Opera. Vol. I Praeparationis Evangelicae Libri I-X.* G B Teubner.

Eichholz D. E., translator (1962). *Pliny: Natural History, In Ten Volumes, X, Libri XXXVI-XXXVII.* Harvard University Press.

Faraone C. A. (2014). "Inscribed Greek Thunderstones as House- and Body-Amulets in Roman Imperial Times". *Kernos (Online)*, **27**, 1–27.

Gaifman M. (2010). "Aniconism and the Notion of the "Primitive" in Greek Antiquity". In Mylonopoulos J., editor, *Divine Images and Human Imaginations in Ancient Greece and Rome.* Brill, pages 63–86.

Gifford E. H., translator (1903). *Eusebii Pamphili: Evangelicae Praeparationis - Libri VI.* Oxford University Press.

Grudem W., editor (2008). *ESV Study Bible: English Standard Version*. Crossway Bibles.

Hendrix H. V., McBeath A., and Gheorghe A. D. (2012). "Meteor Beliefs Project: Spears of God". *WGN, Journal of the IMO*, **40:2**, 80–84.

Johnson D., Tyldesley J., Lowe T., Withers P. J., and Grady M. M. (2013). "Analysis of a prehistoric Egyptian iron bead with implications for the use and perception of meteorite iron in ancient Egypt". *Meteoritics & Planetary Science*, **48:6**, 997–1006.

Knöfel A. and Rendtel J. (1994). "Chladni and the Cosmic Origin of Fireballs and Meteorites, Two Hundred Years of Meteor Astronomy and Meteorite Science". *WGN, Journal of the IMO*, **22:6**, 217–219.

Konuk K. (1998). "The Early Coinage of Kaunos". In Ashton R. and Hurter S., editors, *Studies in Greek Numismatics in Memory of Martin Jessop Price*. London, pages 197–223 & Plates 47–50.

Larsen K., McBeath A., and Gheorghe A. D. (2012). "Meteor Beliefs Project: Meteoritic weapons". In Gyssens M. and Roggemans P., editors, *Proceedings of the International Meteor Conference, Sibiu, Romania, 15-16 September 2011*. IMO, pages 137–144.

LiDonnici L. R. (2001). "Single-Stemmed Wormwood, Pine Cones and Myrrh: Expense and Availability of Recipe Ingredients in the *Greek Magical Papyri*". *Kernos (Online)*, **14**, 61–91.

Lodwick L. (2015). "Identifying Ritual Deposition of Plant Remains: A Case Study of Stone Pine Cones in Roman Britain". In Brindle T., Allen M., Durham E., and Smith A., editors, *TRAC 2014: Proceedings of the Twenty-Fourth Annual Theoretical Roman Archaeology Conference, Reading 2014*. Oxbow Books, pages 54–69.

McBeath A. and Gheorghe A. D. (2004). "Meteor Beliefs Project: The Palladium in ancient and early Medieval sources". *WGN, Journal of the IMO*, **32:4**, 117–121.

McBeath A. and Gheorghe A. D. (2005). "Meteor Beliefs Project: Meteorite worship in the ancient Greek and Roman worlds". *WGN, Journal of the IMO*, **33:5**, 135–144.

McBeath A. and Gheorghe A. D. (2009). "Meteor Beliefs Project: The Tauric Artemis in Classical times". *WGN, Journal of the IMO*, **37:4**, 130–132.

Moore G. F. (1903). "Baetylia". *American Journal of Archaeology*, **7:2**, 198–208.

Oakley K. P. (1971). "The Diopet of Ephesus". *Folklore*, **82:3**, 207–211.

Paton W. R., translator (1922). *Polybius: The Histories II*. William Heinemann & G. P. Putnam's Sons.

Pearse R. (2020). `https://www.tertullian.org/rpearse/mithras/index.htm`. (Mithras pages on the Tertullian.org website).

Pritchard J. B., editor (1969). *Ancient Near Eastern Texts, Relating to the Old Testament. Third Edition with Supplement*. Princeton University Press.

Robinson J. D. (2010). *The Pseudo-Meteoritic Events of the British Isles*. James D Robinson.

Scheyhing N. (2018). "Fossilizing the Holy: Aniconic standing stones of the ancient Near East". In Nebelsick L. D., Wawrzeniuk J., and Zeman-Wiśniewska K., editors, *Archaeologica Hereditas 13: Sacred Space: Contributions to the Archaeology of Belief*. Institute of Archaeology, University of Warsaw, pages 95–112.

Sibley J. T. (2020). "Was Mithras "born" from a meteorite?". *WGN, Journal of the IMO*, **48:1**, 21–24.

Talbert R. J. A., editor (2000). *Barrington Atlas of the Greek and Roman World*. Princeton University Press.

Ulansey D. (1989). *The Origins of the Mithraic Mysteries*. Oxford University Press.

van der Toorn K., Becking B., and van der Horst P. W., editors (1999). *Dictionary of Deities and Demons in the Bible (Second Edition)*. Brill.

Vermaseren M. J. (1956). *Corpus Inscriptionum et Monumentorum Religionis Mithriacae*. Martinus Nijhoff.

Wainwright G. A. (1936). "The coming of iron". *Antiquity*, **10:37**, 5–24.

Handling Editor: Javor Kac

This paper has been typeset from a LaTeX file prepared by the author.

The International Meteor Organization

www.imo.net

Follow us on Facebook InternationalMeteorOrganization

Follow us on Twitter @IMOMeteors

Council

President: Cis Verbeeck,
Bogaertsheide 5, 2560 Kessel, Belgium.
e-mail: cis.verbeeck@scarlet.be

Vice-President: Juraj Tóth,
Fac. Math., Phys. & Inf., Comenius Univ.,
Mlynska dolina, 84248 Bratislava, Slovakia.
e-mail: toth@fmph.uniba.sk

Secretary-General: Robert Lunsford,
14884 Quail Valley Way, El Cajon,
CA 92021-2227, USA. tel. +1 619 755 7791
e-mail: lunro.imo.usa@cox.net

Treasurer: Marc Gyssens, Heerbaan 74,
B-2530 Boechout, Belgium.
e-mail: marc.gyssens@uhasselt.be
BIC: GEBABEBB
IBAN: BE30 0014 7327 5911
Bank transfer costs are always at your expense.

Other Council members:
Javor Kac (see details under WGN)
Detlef Koschny, Zeestraat 46,
NL-2211 XH Noordwijkerhout, Netherlands.
e-mail: detlef.koschny@esa.int
Sirko Molau, Abenstalstraße 13b, D-84072
Seysdorf, Germany. e-mail: sirko@molau.de
Francisco Ocaña Gonzalez, C/ Arquitectura, 7.
28005 Madrid, Spain.
e-mail: francisco.ocana.gonzalez@gmail.com
Vincent Perlerin, 16, rue Georges Bernanos,
51100 Reims, France.
e-mail: vperlerin@gmail.com
Jean-Louis Rault, Société Astronomique de
France, 16, rue de la Vallée, 91360 Epinay sur
Orge, France. e-mail: f6agr@orange.fr
Jürgen Rendtel, Eschenweg 16, D-14476
Marquardt, Germany. e-mail: jrendtel@aip.de

Commission Directors

Visual Commission: Rainer Arlt (rarlt@aip.de)
Generic e-mail address: visual@imo.net
Electronic visual report form:
http://www.imo.net/visual/report/electronic
Video Commission: Sirko Molau (video@imo.net)
Photographic Commission: Bill Ward
(William.Ward@glasgow.ac.uk)
Generic e-mail address: photo@imo.net
Radio Commission: Jean-Louis Rault
(radio@imo.net)
Fireballs: Online fireball reports:
http://fireballs.imo.net

Webmaster

Karl Antier, e-mail: webmaster@imo.net

WGN

Editor-in-chief: Javor Kac
Na Ajdov hrib 24, SI-2310 Slovenska Bistrica,
Slovenia. e-mail: wgn@imo.net;
include METEOR in the e-mail subject line

Editorial board: Ž. Andreić, M. Argo, D.J. Asher,
F. Bettonvil, J. Correira, M. Gyssens,
C. Hergenrother, T. Heywood, J.-L. Rault,
J. Rendtel, C. Verbeeck, S. de Vet, D. Vida.

IMO Sales

Available from the Treasurer or the Electronic Shop on the IMO Website	€	$
IMO membership, including subscription to WGN Vol. 48 (2020)		
Surface mail	26	32
Air Mail (outside Europe only)	49	60
Electronic subscription only	21	25
Proceedings of the International Meteor Conference on paper		
1990, 1991, 1993, 1995, 1996, 1999, 2000, 2002, 2003, per year	9	12
2007, 2010, 2011, per year	15	20
2012, 2013, 2014, 2015 per year	25	34
Proceedings of the Meteor Orbit Determination Workshop 2006	15	20
Radio Meteor School Proceedings 2005	15	20
Handbook for Meteor Observers	15	20
Meteor Shower Workbook	12	16
Electronic media		
Meteor Beliefs Project ZIP archive	6	8

2020 Perseids from Slovakia